A SunCam online continuing education course

Vibration - Modal Analysis

by

Tony L. Schmitz, PhD

1. Modal Analysis

Let's begin our discussion with a definition: *modal analysis is [the] study of the dynamic properties of structures under vibrational excitation* [1]. This may lead us to think of the dynamics of structures such as automobiles, aircraft, spacecraft, and other large complicated systems. A famous example of the importance of considering the dynamics of civil structures is the Tacoma Narrows bridge in Washington state that collapsed in 1940. It failed when the (steady) wind blowing over the bridge caused self-excited vibration, or flutter, in a twisting mode about its centerline; see Fig. 1.1.

Modal analysis is [the] study of the dynamic properties of structures under vibrational excitation [1].

However, even the most common, everyday object has its own dynamic response. For example, sports equipment, including golf clubs and baseball bats, are subject to vibration due to the impulsive force applied during contact with the ball. Rotating equipment, such as fans and washing machines, can exhibit large vibrations when there is an imbalance in the rotating member. This represents forced vibration. Vibration of three bones within the middle ear play a critical role in transforming sound waves into what we perceive as "sound". Here we have an example of free vibration. Regardless of the object's size, shape, or function, we characterize the vibration behavior using a few special descriptors, including natural frequency, mode shape, and frequency response function. A primary objective of this lesson

Figure 1.1: Photograph of the Tacoma Narrows bridge taken prior to its collapse [2].

is to explore these concepts in detail.

We may also consider modal analysis to be the experimental companion of finite element analysis (FEA). While FEA has become an essential tool to aid designers at the modeling stage, it is very often necessary to validate the results. In particular, experimental modal analysis results can be used to confirm decisions about boundary conditions, material properties, and mesh density.

> Important concepts in modal analysis are **natural frequency**, **mode shape**, and **frequency response function**.

In this lesson, we will begin with a review of the fundamentals of single and two degree of freedom free and forced vibrations and, in doing so, we will establish notation conventions for a description of modal analysis. This will provide us with the basis we need to describe techniques for frequency response function measurement and model development.

1.1 Single degree of freedom free vibration

The vibration of bodies that possess both mass and elasticity, or the ability to deform without permanently changing shape, can be divided into three main categories: free, forced, and self-excited vibrations.

> The three categories of vibration are: **free**, **forced**, and **self-excited**.

Free vibration

Free vibration occurs in the absence of a long term, external excitation force. It is the result of some initial conditions imposed on the system, such as a displacement from the system's equilibrium position. Free vibration produces motion in one or more of the system's natural frequencies and, because all physical structures exhibit some form of damping (or energy dissipation), it is seen as a decaying oscillation with a relatively short duration; see Fig. 1.1.1.

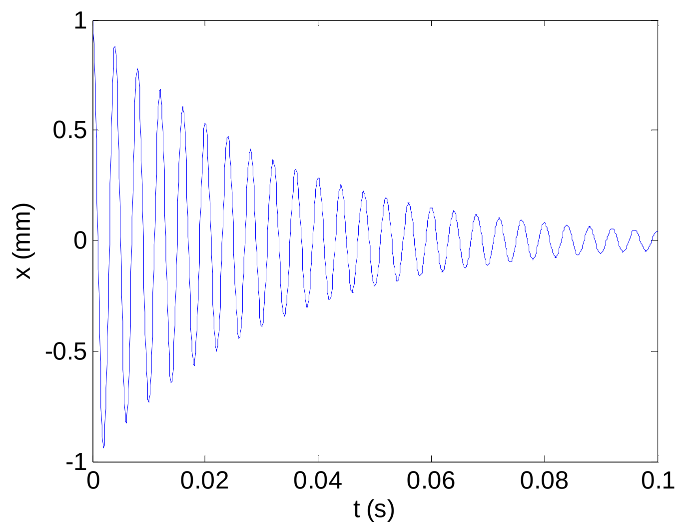

Figure 1.1.1: Damped free vibration example.

Familiar examples include plucking a guitar string or striking a tuning fork.

Forced vibration

Forced vibration takes place when a continuous, external periodic excitation produces a response with the same frequency as the forcing function (after the decay of initial transients). While free vibration is often represented in the time domain, forced vibration is typically analyzed in the frequency domain. This emphasizes the magnitude and phase dependence on frequency and enables the convenient identification of natural frequencies. A typical source of forced vibration in mechanical systems is rotating imbalance. Large vibrations occur when the forcing frequency, ω, is near a system natural frequency, ω_n, as shown in Fig. 1.1.2. This condition is referred to as resonance and is generally avoided.

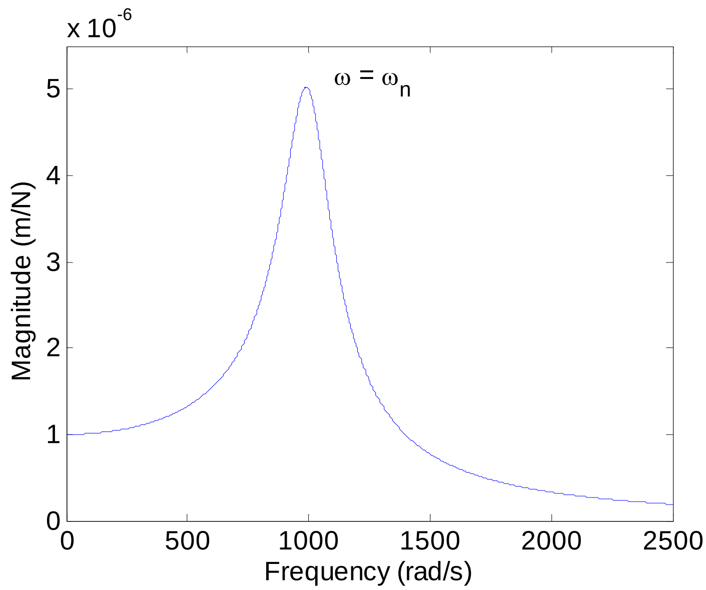

Figure 1.1.2: Example of forced vibration magnitude.

Self-excited vibration

In self-excited vibration, a steady input force is present, as in the case of forced vibration. However, this input is modulated into vibration at one of the system's natural frequencies, as with free vibration. The physical mechanisms that provide this modulation are varied. Common examples of self-excited vibration include playing a violin, flutter in airplane wings (or bridges, as shown in Fig. 1.1), and chatter in machining.

Let's begin our discussion of single degree of freedom free vibration with a simple, lumped parameter model. In this model, all the mass is assumed to be concentrated at the coordinate location and the spring that provides the oscillating restoring force is massless. The model is composed of a mass, m, attached to a linear spring, k, that provides a force proportional to its displacement from the mass's static equilibrium position. Because the rigid mass is only allowed to move vertically, a single time dependent coordinate, x, is sufficient to describe its motion. See Fig. 1.1.3, which includes the free body diagram. Summing the spring and inertial forces in the vertical direction yields the model's equation of motion:

$$m\ddot{x} + kx = 0\,. \tag{1.1.1}$$

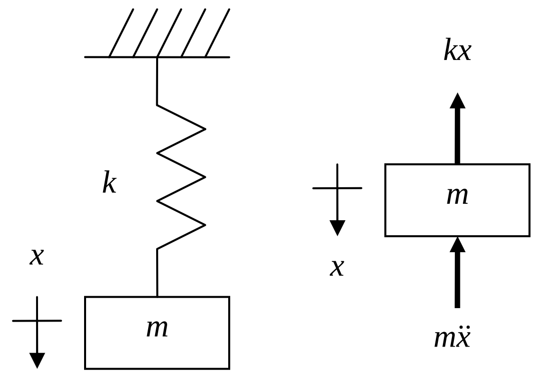

Figure 1.1.3: Single degree of freedom, undamped lumped parameter model (left); free body diagram (right).

By assuming a harmonic solution of the form $x = Xe^{st}$, where X is a complex coefficient, $s = i\omega$, and ω is the frequency (in rad/s), we can express the velocity as the first time derivative of the displacement, $\dot{x} = sXe^{st} = i\omega Xe^{st}$, and the acceleration as the second time derivative, $\ddot{x} = s^2 Xe^{st} = -\omega^2 Xe^{st}$ (note that $i = \sqrt{-1}$ and $i^2 = -1$). Substitution into Eq. 1.1.1 gives:

$$Xe^{st}\left(ms^2 + k\right) = 0. \qquad (1.1.2)$$

In this equation, either Xe^{st} or $\left(ms^2 + k\right)$ is zero. If the first term is zero, this means that no motion has occurred and it is described as the trivial solution. We are interested in the case that the second term is equal to zero. This is referred to as the characteristic equation for the system:

$$ms^2 + k = 0. \qquad (1.1.3)$$

Solving for the complex variable s gives the two roots $s = \pm\sqrt{-\frac{k}{m}} = \pm i\sqrt{\frac{k}{m}}$. The vibrating frequency $\sqrt{\frac{k}{m}} = \omega_n$ is the **natural frequency** for the single degree of freedom system. Typical SI units for k and m are N/m and kg, respectively, which gives units of rad/s for ω_n.

Alternately, the natural frequency may be expressed in units of Hz (cycles/s). In this case, we'll use the notation $f_n = \frac{\omega_n}{2\pi}$.

The total solution to Eq. 1.1.1 is the sum of the contributions from each of the two roots:

$$x = X_1 e^{i\omega_n t} + X_2 e^{-i\omega_n t}. \qquad (1.1.4)$$

The complex coefficients, X_1 and X_2, can be determined from the initial displacement, x_0, and velocity, $\dot{x}_0$, of the single degree of freedom system. Evaluating Eq. 1.1.4 at $t = 0$ gives:

$$x_0 = X_1 + X_2. \qquad (1.1.5)$$

The first time derivative of Eq. 1.1.4 is:

$$\dot{x} = i\omega_n X_1 e^{i\omega_n t} - i\omega_n X_2 e^{-i\omega_n t}. \qquad (1.1.6)$$

At $t = 0$, Eq. 1.1.6 becomes:

$$\dot{x}_0 = i\omega_n X_1 - i\omega_n X_2. \qquad (1.1.7)$$

Equations 1.1.5 and 1.1.7 can be combined to determine the complex conjugate coefficients X_1 and X_2:

$$X_1 = \frac{-i\dot{x}_0 + \omega_n x_0}{2\omega_n} \text{ and} \qquad (1.1.8)$$

$$X_2 = \frac{i\dot{x}_0 + \omega_n x_0}{2\omega_n}. \qquad (1.1.9)$$

These coefficients can then be substituted in Eq. 1.1.4 to determine the time dependent displacement of the mass due to the imposed initial conditions. Alternately, the mass motion can be expressed in exponential form. To use this notation, we first need to identify the real (Re) and imaginary (Im) parts of the complex coefficients:

$$\mathrm{Re}(X_1) = \frac{x_0}{2} \qquad \mathrm{Im}(X_1) = \frac{-\dot{x}_0}{2\omega_n} \tag{1.1.10}$$

$$\mathrm{Re}(X_2) = \frac{x_0}{2} \qquad \mathrm{Im}(X_2) = \frac{\dot{x}_0}{2\omega_n}. \tag{1.1.11}$$

These real and imaginary parts can then be used to write the coefficients in exponential form:

$$X_1 = Ae^{i\beta} = \sqrt{\mathrm{Re}(X_1)^2 + \mathrm{Im}(X_1)^2}\,\exp\left(i \cdot \tan^{-1}\left(\frac{\mathrm{Im}(X_1)}{\mathrm{Re}(X_1)}\right)\right)$$

$$X_1 = \sqrt{\left(\frac{x_0}{2}\right)^2 + \left(\frac{-\dot{x}_0}{2\omega_n}\right)^2}\,\exp\left(i \cdot \tan^{-1}\left(\frac{\frac{-\dot{x}_0}{2\omega_n}}{\frac{x_0}{2}}\right)\right) \tag{1.1.12}$$

$$X_1 = \sqrt{\frac{{x_0}^2{\omega_n}^2 + {\dot{x}_0}^2}{4{\omega_n}^2}}\,\exp\left(i \cdot \tan^{-1}\left(-\frac{\dot{x}_0}{x_0\omega_n}\right)\right)$$

where the magnitude is $A = \sqrt{\frac{{x_0}^2{\omega_n}^2 + {\dot{x}_0}^2}{4{\omega_n}^2}}$ and the phase is $\beta = \tan^{-1}\left(-\frac{\dot{x}_0}{x_0\omega_n}\right)$. Similarly, $X_2 = Ae^{-i\beta}$ (same magnitude, but negative phase) because it is the complex conjugate of X_1. We can then rewrite the total solution from Eq. 1.1.4 in the form:

$$x = Ae^{i\beta}e^{i\omega_n t} + Ae^{-i\beta}e^{-i\omega_n t} = A\left(e^{i(\omega_n t+\beta)} + e^{-i(\omega_n t+\beta)}\right). \tag{1.1.13}$$

Finally, by applying the Euler identity $e^{i\theta} + e^{-i\theta} = 2\cos(\theta)$, Eq. 1.1.13 can be rewritten as:

$$x = 2A\cos(\omega_n t + \beta). \tag{1.1.14}$$

While Eq. 1.1.14 emphasizes the oscillatory nature of the mass motion and the dependence of the magnitude and phase on the initial conditions, we must also include damping in our analysis in order to model physical systems. Damping refers to the "leakage" of the input energy into the vibrating system. In other words, not all of the input energy serves to cause motion. Some of it is dissipated in other ways. A comprehensive model of damping is complicated and not particularly well suited for incorporation into our simple mathematical description of single degree of freedom free vibration. Therefore, one or more of three mathematically simple, but effective, damping models are typically applied.

> **Damping** refers to the "leakage" of the input energy into the vibrating system.

Viscous damping

A common assertion is that the retarding damping force is proportional to the mass velocity. You may have experienced this phenomenon if you've attempted to force a body through a fluid, such as pulling your hand through water or sticking your hand out the window of a moving vehicle. You probably observed that increasing the speed of your hand relative to the fluid raised the resistance proportionally. If we write the damping force as:

$$f = c\dot{x} \tag{1.1.15}$$

and substitute the velocity expression $\dot{x} = sXe^{st} = i\omega Xe^{st}$, we see that viscous damping is frequency dependent. When sketching models of lumped parameter systems, the damping element is often illustrated as a fluid dashpot (similar to a car's shock absorber) when the viscous damping model is applied. Typical SI units for *c* are N-s/m.

Coulomb damping

Another effective damping model is Coulomb damping, or dry sliding friction. Here, energy is dissipated (as heat) due to relative motion between two contacting surfaces. The force magnitude depends on the sliding (kinetic) friction coefficient, μ, and the normal force, *N*, between the two bodies. See Fig. 1.1.4. Because the friction force always opposes the direction of motion, the resulting equation of motion is nonlinear. A piecewise definition[1] of the Coulomb damping force is [3]:

[1] A piecewise definition is one with separate, non-overlapping, parts.

$$f = \begin{Bmatrix} -\mu N & \dot{x} > 0 \\ 0 & \dot{x} = 0 \\ \mu N & \dot{x} < 0 \end{Bmatrix}. \qquad (1.1.16)$$

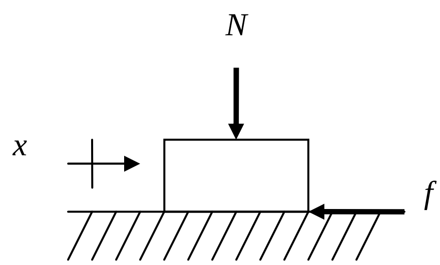

Figure 1.1.4: Coulomb damping occurs due to dry sliding friction between the two surfaces. The normal and friction forces are shown.

Solid damping

Even in the absence of an external fluid medium or sliding friction against another surface, the motion of a freely oscillating body decays over time. This is due to energy dissipation internal to the body (perhaps a good mental picture is molecules sliding relative to each other within the body itself during periodic motion and elastic deformation). The energy dissipation during a cycle of motion for this solid or structural damping is taken to be proportional to the square of the vibration magnitude. Using the concept of equivalent viscous damping, solid damping is often incorporated with stiffness to arrive at a complex stiffness term in the differential equation of motion [4].

For the remainder of this lesson, we will use viscous damping to describe energy dissipation in the lumped parameter models. The equation of motion for free vibration of the single degree of freedom spring-mass-damper (Fig. 1.1.5) can then be written as:

$$m\ddot{x} + c\dot{x} + kx = 0\,. \qquad (1.1.17)$$

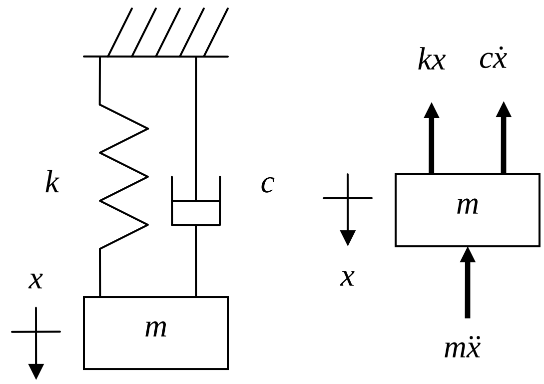

Figure 1.1.5: Single degree of freedom, damped lumped parameter model (left); free body diagram (right).

Again assuming the harmonic solution $x = Xe^{st}$, we obtain the characteristic equation:

$$ms^2 + cs + k = 0, \tag{1.1.18}$$

which can be rewritten as:

$$s^2 + \frac{c}{m}s + \frac{k}{m} = 0. \tag{1.1.19}$$

This equation is quadratic in s^2 and has the two roots:

$$s_{1,2} = -\frac{c}{2m} \pm \sqrt{\left(\frac{c}{2m}\right)^2 - \frac{k}{m}}. \tag{1.1.20}$$

The vibratory behavior of the spring-mass-damper depends on the term under the radical in Eq. 1.1.20. If $\left(\frac{c}{2m}\right)^2 - \frac{k}{m} < 0$, the system is underdamped and vibratory. If $\left(\frac{c}{2m}\right)^2 - \frac{k}{m} = 0$, the system is said to be critically damped and, if $\left(\frac{c}{2m}\right)^2 - \frac{k}{m} > 0$, then the system is overdamped. For these two cases, no vibration (oscillation) occurs. Because the damping is generally low in mechanical systems, we will consider only the underdamped option in our analyses. For underdamped systems, Eq. 1.1.20 can be rewritten as:

$$s_{1,2} = -\zeta\omega_n \pm i\omega_d, \tag{1.1.21}$$

> Mechanical systems can be underdamped, critically damped, or overdamped. Most systems are **underdamped**, which means that they will oscillate during free vibration.

where we've introduced the dimensionless damping ratio, $\zeta = \frac{c}{2\sqrt{km}}$, and damped natural frequency, $\omega_d = \omega_n\sqrt{1-\zeta^2}$. Under the viscous damping assumption, we see that the free vibrating frequency is reduced in the presence of damping. However, for typical mechanical systems, the damping is low enough that the frequency change is negligible. Using the two roots in Eq. 1.1.21, the total solution for the free motion of the single degree of freedom spring-mass-damper is:

$$x = X_1 e^{(-\zeta\omega_n + i\omega_d)t} + X_2 e^{(-\zeta\omega_n - i\omega_d)t} = e^{-\zeta\omega_n t}\left(X_1 e^{i\omega_d t} + X_2 e^{-i\omega_d t}\right). \tag{1.1.22}$$

Like the undamped case, the complex coefficients can be determined from the initial conditions. Taking the time derivative of Eq. 1.1.22, substituting the initial displacement, x_0, and velocity, $\dot{x}_0$, and solving for X_1 and X_2 gives the complex conjugate pair:

$$X_1 = \frac{x_0}{2} - i\frac{\dot{x}_0 + \zeta\omega_n x_0}{2\omega_d} \text{ and } X_2 = \frac{x_0}{2} + i\frac{\dot{x}_0 + \zeta\omega_n x_0}{2\omega_d}. \tag{1.1.23}$$

Using these coefficients, the exponential form can again be developed in a similar way to Eq. 1.1.12 by substituting for the real and imaginary parts. For example, $\mathrm{Re}(X_1) = \frac{x_0}{2}$ and $\mathrm{Im}(X_1) = -\frac{\dot{x}_0 + \zeta\omega_n x_0}{2\omega_d}$ for the coefficient X_1. Note that these terms simplify to Eq. 1.1.10 for the undamped case if ζ is set equal to zero.

1.2 Single degree of freedom forced vibration

We will again consider the spring-mass-damper model shown in Fig. 1.1.5. However, a harmonic external force is now applied to the mass. The force is shown as $fe^{i\omega t}$ in Fig. 1.2.1. The corresponding equation of motion is:

$$m\ddot{x} + c\dot{x} + kx = f \ . \qquad (1.2.1)$$

Although the total solution to Eq. 1.2.1 includes both the homogeneous (transient) and particular (steady state) components, we have already described the damped transient response in the previous section. We will therefore consider only the steady state solution here. Because the motion response has the same frequency as the forcing function, we can assume a solution of the form $x = Xe^{i\omega t}$. The velocity and acceleration can then be written as $\dot{x} = i\omega Xe^{i\omega t}$ and $\ddot{x} = -\omega^2 Xe^{i\omega t}$. Substituting in Eq. 1.2.1 gives:

$$\left(-\omega^2 m + i\omega c + k\right)Xe^{i\omega t} = fe^{i\omega t} \ . \qquad (1.2.2)$$

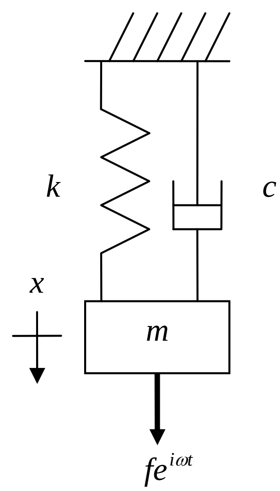

Figure 1.2.1: Single degree of freedom, lumped parameter model (damped with force).

Rewriting Eq. 1.2.2 gives the complex valued **frequency response function (FRF)**. We will use this description of Eq. 1.2.3, rather than transfer function, because we can only consider

> The total solution to forced vibration includes both transient and steady state components.

positive frequencies and a single system configuration (damping and natural frequency) when we perform measurements. The term transfer function refers to the theoretical situation where all frequencies ($-\infty$ to $+\infty$) and $\zeta\omega_n$ combinations are included.

$$\frac{X}{F} = \frac{1}{-m\omega^2 + ic\omega + k} \tag{1.2.3}$$

There are two primary ways to represent the complex function shown in Eq. 1.2.3. The first is to separate the function into its magnitude and phase components and the second is to express the function using its real and imaginary parts. The frequency dependent magnitude and phase are written as:

$$\left|\frac{X}{F}\right| = \frac{1}{k}\sqrt{\frac{1}{\left(1-\left(\frac{\omega}{\omega_n}\right)^2\right)^2 + \left(2\zeta\frac{\omega}{\omega_n}\right)^2}} \quad \text{and} \tag{1.2.4}$$

$$\Phi = \tan^{-1}\left(\frac{\mathrm{Im}\left(\frac{X}{F}\right)}{\mathrm{Re}\left(\frac{X}{F}\right)}\right) = \tan^{-1}\left(\frac{-2\zeta\frac{\omega}{\omega_n}}{1-\left(\frac{\omega}{\omega_n}\right)^2}\right). \tag{1.2.5}$$

Because Eqs. 1.2.4 and 1.2.5 are somewhat cumbersome, it is common to replace the frequency ratio $\frac{\omega}{\omega_n}$ with another variable, such as *r*. We will also adopt this convention. The real and imaginary parts of the FRF are provided in Eqs. 1.2.6 and 1.2.7.

$$\mathrm{Re}\left(\frac{X}{F}\right) = \frac{1}{k}\left(\frac{1-r^2}{\left(1-r^2\right)^2 + \left(2\zeta r\right)^2}\right) \tag{1.2.6}$$

$$\mathrm{Im}\left(\frac{X}{F}\right) = \frac{1}{k}\left(\frac{-2\zeta r}{\left(1-r^2\right)^2 + \left(2\zeta r\right)^2}\right) \tag{1.2.7}$$

<u>Example 1.2.1: FRF for single degree of freedom system</u>

Let's consider a single degree of freedom spring-mass-damper system with a mass of 1 kg, a spring constant of 1×10^{6} N/m, and a viscous damping coefficient of 200 N-s/m. In order to apply Eqs. 1.2.4-1.2.7, we must calculate the (undamped) natural frequency and damping ratio.

$$\omega_n = \sqrt{\frac{k}{m}} = \sqrt{\frac{1\times10^{6}}{1}} = 1000 \text{ rad/s}$$

$$\zeta = \frac{c}{2\sqrt{km}} = \frac{200}{2\sqrt{1\times10^{6}\cdot 1}} = 0.1$$

Figure 1.2.2 shows the magnitude and phase as a function of the frequency ratio, r. Although a logarithmic magnitude axis (i.e., a semilog plot) is often shown in the literature, we will use a linear convention for plots unless specified otherwise. The real and imaginary parts are provided in Fig. 1.2.3. Note that the zero frequency (DC) value for both the real part and magnitude is $\frac{1}{k} = 1\times10^{-6}$ m/N. This represents the real valued static deflection of the spring (away from its equilibrium position) under a unit force. We can also see that the magnitude at resonance ($r = 1$ or $\omega = \omega_n$) is significantly larger than the DC deflection. This magnitude is $\frac{1}{2k\zeta} = 5\times10^{-6}$ m/N.

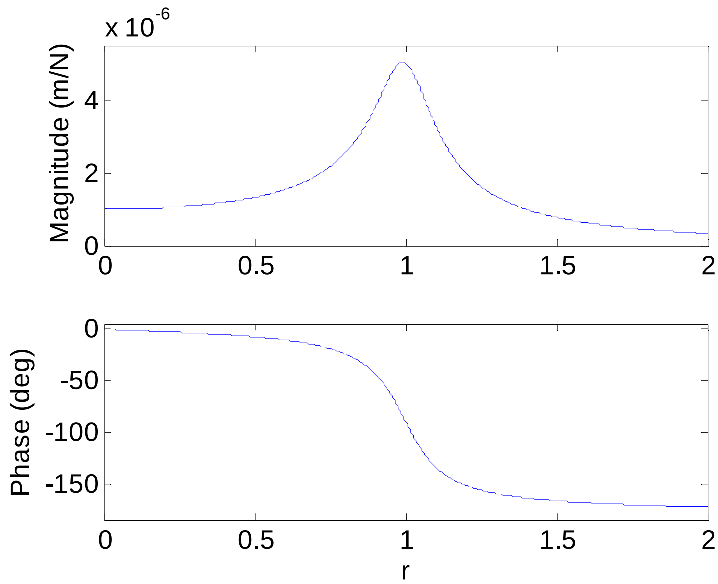

Figure 1.2.2: Magnitude and phase for example single degree of freedom system.

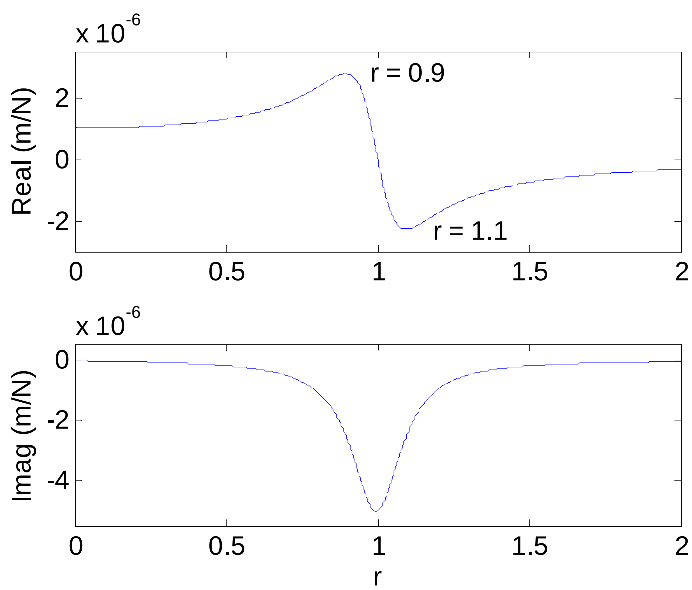

Figure 1.2.3: Real and imaginary parts for example single degree of freedom system.

The maximum value of the real part occurs at $r = \sqrt{1-2\zeta}$, which we will approximate as

$r = 1 - \zeta = 0.9$ (this approximation is valid for small ζ values when ζ^2 is negligible). The minimum real part occurs at $r = \sqrt{1+2\zeta}$, approximated as $r = 1 + \zeta = 1.1$. The difference in the real value between these maximum and minimum points is the same as the magnitude peak value $\frac{1}{2k\zeta} = 5 \times 10^{-6}$ m/N. The imaginary minimum is seen at resonance with a value of $\frac{-1}{2k\zeta} = -5 \times 10^{-6}$ m/N.

In addition to the frequency dependent representations of the FRF shown in Figs. 1.2.2 and 1.2.3, the Argand diagram can also be selected. In this case, the real part is graphed versus the imaginary part (i.e., the complex plane) and the same information identified in the previous paragraphs is compactly represented. As we traverse the "circle" clockwise from $r = 0$, where the real part is $\frac{1}{k} = 1 \times 10^{-6}$ m/N and the imagnary part is zero, we sequentially encounter the $r = 1 - \zeta = 0.9$ point where the real part is maximum, the $r = 1$ point where the real part is zero and the imaginary part is most negative, the $r = 1 + \zeta = 1.1$ point where the real part is most negative, and, finally, we approach the $r = \infty$ frequency ratio where both the real and imaginary parts are zero.

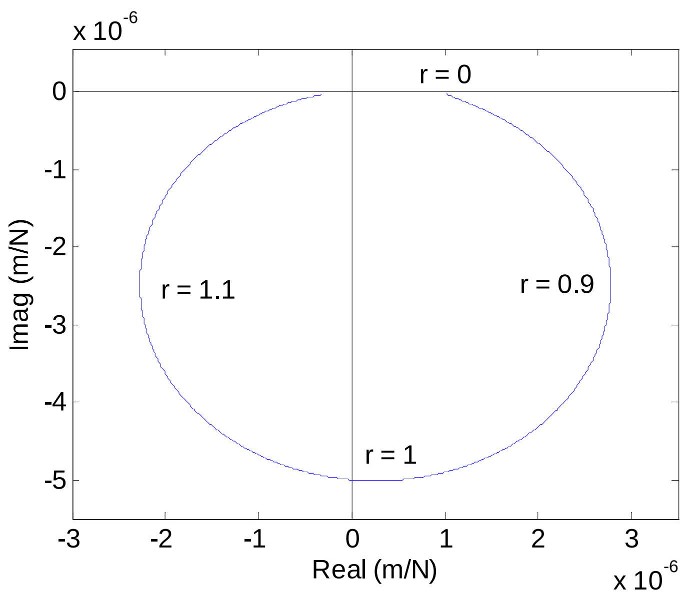

Figure 1.2.4: Argand diagram for example single degree of freedom system.

Using a vector representation for $\frac{X}{F}$, the magnitude is identified as the length of the vector which extends from the origin to any point (i.e., a desired *r* value) on our "circle". The phase lag between the displacement and force is the angle between the vector and the positive real axis. The real and imaginary parts are simply the projections of the vector on the real and imaginary axes.

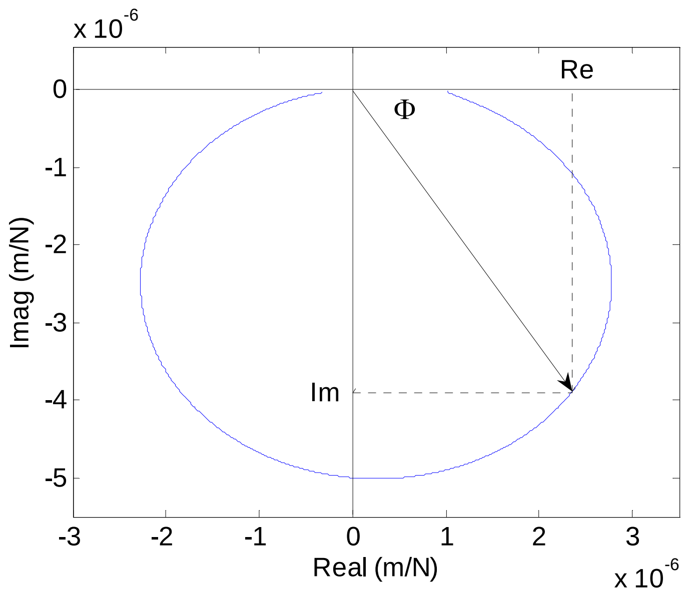

Figure 1.2.5: Vector representation of FRF in the complex plane.

1.3 Two degree of freedom free vibration

We will again use the lumped parameter spring-mass-damper model as the basis for our discussion, but we will now include a second degree of freedom by adding a second spring-mass-damper to the first in a "chain-type" configuration; see Fig. 1.3.1. Using the free body diagrams for the top and bottom masses, where inertial forces are shown in addition to the spring and viscous damper forces, the two equations of motion can be written by equating the sum of the forces in the vertical direction to zero. The equation of motion for the top mass is:

$$m_1\ddot{x}_1 + (c_1 + c_2)\dot{x}_1 + (k_1 + k_2)x_1 - c_2\dot{x}_2 - k_2x_2 = 0 \tag{1.3.1}$$

and the equation of motion for the bottom mass is:

$$m_2\ddot{x}_2 - c_2\dot{x}_1 - k_2x_1 + c_2\dot{x}_2 + k_2x_2 = 0\,. \qquad (1.3.2)$$

> Modal analysis enables us to uncouple the equations of motion for multiple degree of freedom systems so that we can use our single degree of freedom solution techniques.

The difference we may observe between the single and two degree of freedom situations is that, for the two degree of freedom case, the equations of motion are coupled; they both contain the displacements x_1 and x_2 and velocities $\dot{x}_1$ and $\dot{x}_2$. This complicates the system solution and provides the motivation for modal analysis, which enables us to uncouple these two equations through a coordinate transformation and then use our single degree of freedom solution techniques. Before describing this approach, however, let's continue with our discussion of the chain-type two degree of freedom model.

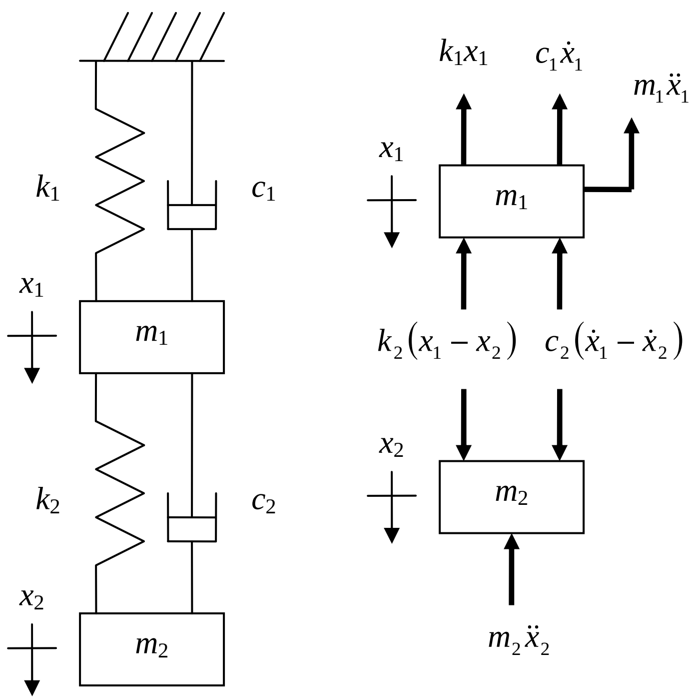

Figure 1.3.1: Two degree of freedom, damped lumped parameter model (left); free body diagram (right).

The equations of motion are compactly expressed using a matrix formulation:

$$\begin{bmatrix} m_1 & 0 \\ 0 & m_2 \end{bmatrix}\begin{Bmatrix} \ddot{x}_1 \\ \ddot{x}_2 \end{Bmatrix} + \begin{bmatrix} c_1 + c_2 & -c_2 \\ -c_2 & c_2 \end{bmatrix}\begin{Bmatrix} \dot{x}_1 \\ \dot{x}_2 \end{Bmatrix} + \begin{bmatrix} k_1 + k_2 & -k_2 \\ -k_2 & k_2 \end{bmatrix}\begin{Bmatrix} x_1 \\ x_2 \end{Bmatrix} = \begin{Bmatrix} 0 \\ 0 \end{Bmatrix}. \qquad (1.3.3)$$

The coupling is seen to occur in the symmetric damping and stiffness matrices for this chain-type model due to the nonzero off-diagonal terms in the matrix positions (1,2) and (2,1). If we represent the mass and stiffness matrices as $[M]$ and $[K]$, neglect damping for now, and assume a harmonic solution of the form $x = Xe^{st}$, we can write:

$$\left([M]s^2 + [K]\right)\{X\}e^{st} = \{0\}. \qquad (1.3.4)$$

Similar to Eq. 1.1.2, there are two possibilities for the product in Eq. 1.3.4. If $\{X\} = \{0\}$, we obtain the trivial solution. We are therefore interested in the case when $\left([M]s^2 + [K]\right) = \{0\}$. From linear algebra [5], we know that for this matrix of equations to have a non-trivial solution, the determinant must be equal to zero. This represents the characteristic equation for our system.

$$\left|[M]s^2 + [K]\right| = 0 \qquad (1.3.5)$$

The determinant of a two row, two column (2x2) matrix can be calculated by finding the difference between the products of the on-diagonal (1,1 and 2,2) terms and the off-diagonal terms. This is expressed generically as:

$$\begin{vmatrix} as^2 + b & cs^2 + d \\ cs^2 + d & es^2 + f \end{vmatrix} = 0 \text{ or} \qquad (1.3.6)$$

$$\left(as^2 + b\right)\left(es^2 + f\right) - \left(cs^2 + d\right)^2 = 0. \qquad (1.3.7)$$

This equation is quadratic in s^2, i.e., $gs^4 + hs^2 + m = 0$, and we can find the roots, $s_1^{\,2}$ and $s_2^{\,2}$, using the quadratic equation. These two roots are the eigenvalues for the two degree of freedom system. The **natural frequencies** are calculated as:

$$s_1^{\,2} = -\omega_{n1}^{\,2} \text{ and } s_2^{\,2} = -\omega_{n2}^{\,2}, \qquad (1.3.8)$$

where, by convention, $\omega_{n1} < \omega_{n2}$.

To find the eigenvectors, or **mode shapes**, we substitute $s_1^{\ 2}$ and $s_2^{\ 2}$ into the equation of motion for the top or bottom mass (either will give the same solution because we imposed linear dependence between the two equations when we set the determinant equal to zero in Eq. 1.3.5). The equation of motion for the top mass corresponds to the top row in Eq. 1.3.9; recall that we are ignoring damping for now. See Eq. 1.3.10.

$$\begin{bmatrix} m_1 s^2 + k_1 + k_2 & -k_2 \\ -k_2 & m_2 s^2 + k_2 \end{bmatrix} \begin{Bmatrix} X_1 \\ X_2 \end{Bmatrix} = \begin{Bmatrix} 0 \\ 0 \end{Bmatrix} \tag{1.3.9}$$

$$\left(m_1 s^2 + k_1 + k_2\right) X_1 - k_2 X_2 = 0 \tag{1.3.10}$$

Because the two mode shapes represent the relative magnitude and direction of vibration between the two coordinates in the two degree of freedom system, we want to calculate either the ratio $\frac{X_1}{X_2}$ or $\frac{X_2}{X_1}$. We can choose to normalize the eigenvector to either coordinate x_1 or x_2. In most situations, the coordinate of interest or location of force application is selected. For the chain-type model, if we wish to normalize to coordinate x_1, we require the ratios $\frac{X_1}{X_1} = 1$ and $\frac{X_2}{X_1}$. Using Eq. 1.3.10, we find that $\frac{X_2}{X_1} = \frac{m_1 s^2 + k_1 + k_2}{k_2}$ and the first mode shape is:

Mode shapes represent the relative magnitude and direction of vibration between model coordinates.

$$\psi_1 = \begin{Bmatrix} \frac{X_1}{X_1} \\ \frac{X_2}{X_1} \end{Bmatrix} = \begin{Bmatrix} 1 \\ \frac{m_1 s_1^{\ 2} + k_1 + k_2}{k_2} \end{Bmatrix}. \tag{1.3.11}$$

The second mode shape is determined by substitution of $s_2^{\ 2}$ in place of $s_1^{\ 2}$:

$$\psi_2 = \begin{Bmatrix} \dfrac{X_1}{X_1} \\ \dfrac{X_2}{X_1} \end{Bmatrix} = \begin{Bmatrix} 1 \\ \dfrac{m_1 s_2{}^2 + k_1 + k_2}{k_2} \end{Bmatrix}. \tag{1.3.12}$$

The first mode shape corresponds to vibration in the first natural frequency ω_{n1}, while the second mode shape is associated with vibration at ω_{n2}. In general, the system will vibrate in a linear combination of both mode shapes/natural frequencies, depending on the initial conditions. If we've followed the convention of $\omega_{n1} < \omega_{n2}$ and normalized to the x_1 coordinate, we'll find that the first mode shape will take the form $\psi_1 = \begin{Bmatrix} 1 \\ a > 0 \end{Bmatrix}$, where a is a real number, which indicates that the two masses are vibrating exactly in phase with one another (i.e., they reach their maximum and minimum displacements at the same instants in time). We'll also see that the second mode shape will take the form $\psi_2 = \begin{Bmatrix} 1 \\ a < 0 \end{Bmatrix}$, which means that the mass motions are exactly out of phase with one another (i.e., when one mass reaches its maximum displacement, the other is at its minimum displacement).

> The first mode shape corresponds to vibration in the first natural frequency. The second mode shape oscillates at the second natural frequency and so on.

<u>Example 1.3.1: Free vibration using complex coefficients</u>

In this example we will calculate the time response of the system in Fig. 1.3.1 when the mass values are $m_1 = 1$ kg and $m_2 = 0.5$ kg, the stiffness values are $k_1 = 1\times10^7$ N/m and $k_2 = 2\times10^7$ N/m, the initial displacement of x_1 is $x_{0,1} = 1$ mm and the initial displacement of x_2 is $x_{0,2} = -1$ mm, and the initial velocities are zero. The equations of motion in matrix form are:

$$\begin{bmatrix} 1 & 0 \\ 0 & 0.5 \end{bmatrix}\begin{Bmatrix} \ddot{x}_1 \\ \ddot{x}_2 \end{Bmatrix} + \begin{bmatrix} 1\times10^7 + 2\times10^7 & -2\times10^7 \\ -2\times10^7 & 2\times10^7 \end{bmatrix}\begin{Bmatrix} x_1 \\ x_2 \end{Bmatrix} = \begin{Bmatrix} 0 \\ 0 \end{Bmatrix}.$$

The characteristic equation is:

$$\begin{vmatrix} 1s^2+3\times10^7 & -2\times10^7 \\ -2\times10^7 & 0.5s^2+2\times10^7 \end{vmatrix}=0\text{, or } 0.5s^4+3.5\times10^7 s^2+2\times10^{14}=0.$$

This equation yields the two roots $s_1^{\ 2}=-6.277\times10^6$ (rad/s)^2 and $s_2^{\ 2}=-6.372\times10^7$ (rad/s)^2, which give the natural frequencies $\omega_{n1}=\sqrt{-s_1^{\ 2}}=2505$ rad/s and $\omega_{n2}=\sqrt{-s_2^{\ 2}}=7983$ rad/s. Expressed in units of Hz, these natural frequencies are $f_{n1}=\frac{\omega_{n1}}{2\pi}=398.8$ Hz and $f_{n2}=\frac{\omega_{n2}}{2\pi}=1271$ Hz.

Let's normalize the mode shapes to x_2 and arbitrarily select the equation of motion for the top mass to calculate the ratio $\frac{X_1}{X_2}=\frac{2\times10^7}{1s^2+3\times10^7}$. We obtain the first mode shape, which corresponds to vibration in ω_{n1}, by substituting $s_1^{\ 2}$ in this ratio:

$$\psi_1=\begin{Bmatrix} \frac{X_1}{X_2} \\ \frac{X_2}{X_2} \end{Bmatrix}=\begin{Bmatrix} \frac{2\times10^7}{-6.277\times10^6+3\times10^7} \\ 1 \end{Bmatrix}=\begin{Bmatrix} 0.8431 \\ 1 \end{Bmatrix}.$$

See Fig. 1.3.2, where the relative deflection amplitudes between coordinates 1 and 2 are identified. The second mode shape, which corresponds to vibration in ω_{n2}, is:

$$\psi_2=\begin{Bmatrix} \frac{X_1}{X_2} \\ \frac{X_2}{X_2} \end{Bmatrix}=\begin{Bmatrix} \frac{2\times10^7}{-6.372\times10^7+3\times10^7} \\ 1 \end{Bmatrix}=\begin{Bmatrix} -0.5931 \\ 1 \end{Bmatrix}.$$

See Fig. 1.3.3, where the deflections are now in opposite directions (out of phase). Similar to Eq. 1.1.4, we can generically write the time domain solution for the x_1 and x_2 vibrations as:

$$x_1=X_{11}e^{i2505t}+X_{11}^{\ *}e^{-i2505t}+X_{12}e^{i7983t}+X_{12}^{\ *}e^{-i7983t}\text{ and}$$
$$x_2=X_{21}e^{i2505t}+X_{21}^{\ *}e^{-i2505t}+X_{22}e^{i7983t}+X_{22}^{\ *}e^{-i7983t}.$$

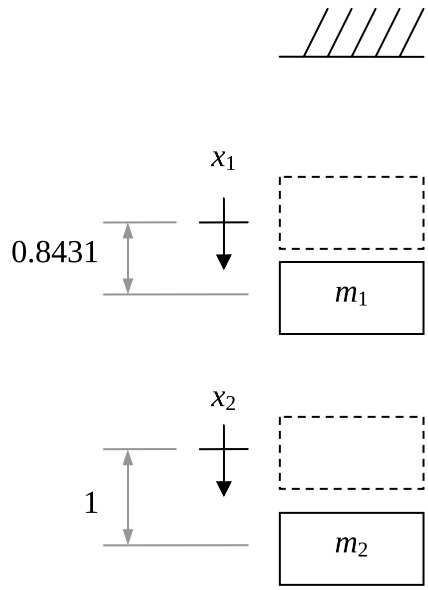

Figure 1.3.2: Mode shape 1
normalized to coordinate 2.

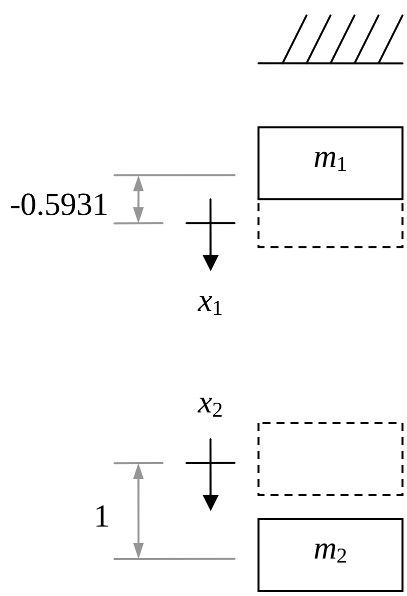

Figure 1.3.3: Mode shape 2
normalized to coordinate 2.

Here, X_{ij} and X_{ij}^* represent a complex conjugate pair, where the subscript *i* indicates the coordinate number and the subscript *j* denotes the natural frequency number. This solution suggests the general case that the total vibration is a linear combination of vibration in each of the two modes. The first time derivatives are:

$$\dot{x}_1 = i2505\left(X_{11}e^{i2505t} - X_{11}^*e^{-i2505t}\right) + i7983\left(X_{12}e^{i7983t} - X_{12}^*e^{-i7983t}\right) \text{ and}$$
$$\dot{x}_2 = i2505\left(X_{21}e^{i2505t} - X_{21}^*e^{-i2505t}\right) + i7983\left(X_{22}e^{i7983t} - X_{22}^*e^{-i7983t}\right).$$

Substitution of the initial conditions leads to a system of four equations with eight unknowns.

$$\begin{aligned} x_{0,1} &= 1 = X_{11} + X_{11}^* + X_{12} + X_{12}^* \\ x_{0,2} &= -1 = X_{21} + X_{21}^* + X_{22} + X_{22}^* \\ \dot{x}_{0,1} &= 0 = i2505\left(X_{11} - X_{11}^*\right) + i7983\left(X_{12} - X_{12}^*\right) \\ \dot{x}_{0,2} &= 0 = i2505\left(X_{21} - X_{21}^*\right) + i7983\left(X_{22} - X_{22}^*\right) \end{aligned}$$

However, we can apply the mode shape relationships to reduce this to a system of four equations with four unknowns. Using the same definitions for the X_{ij} subscripts, we can write $\frac{X_{11}}{X_{21}} = 0.8431$ and $\frac{X_{11}}{X_{21}} = -0.5931$. After substitution and rewriting in matrix form, we obtain:

$$\begin{bmatrix} 0.8431 & 0.8431 & -0.5931 & -0.5931 \\ 1 & 1 & 1 & 1 \\ i2112 & -i2112 & i4734 & -i4734 \\ i2505 & -i2505 & i7983 & -i7983 \end{bmatrix} \begin{Bmatrix} X_{21} \\ X_{21}^* \\ X_{22} \\ X_{22}^* \end{Bmatrix} = \begin{Bmatrix} 1 \\ -1 \\ 0 \\ 0 \end{Bmatrix}, \text{ or } [A]\{X\} = \{b\}.$$

We can determine the coefficients by inverting $[A]$ and premultiplying $\{b\}$ by this result, $\{X\} = [A]^{-1}\{b\}$. The result is $\begin{Bmatrix} X_{21} \\ X_{21}^* \\ X_{22} \\ X_{22}^* \end{Bmatrix} = \begin{Bmatrix} 0.1417 \\ 0.1417 \\ -0.6417 \\ -0.6417 \end{Bmatrix}$. Using these values and the mode shape relationships to obtain the remaining four coefficients, we can substitute in the original x_1 and x_2 expressions to determine the time dependent free vibration for our example system.

$$x_1 = 0.1194e^{i2505t} + 0.1194e^{-i2505t} + 0.3805e^{i7983t} + 0.3805e^{-i7983t}$$
$$x_2 = 0.1417e^{i2505t} + 0.1417e^{-i2505t} - 0.6417e^{i7983t} - 0.6417e^{-i7983t}$$

Further, we can use the Euler identity $e^{i\theta} + e^{-i\theta} = 2\cos(\theta)$ to rewrite x_1 and x_2 as a sum of cosines. It is seen that the final motion of each mass is a linear combination of vibration in the two natural frequencies.

$$x_1 = 0.2388\cos(2505t) + 0.7610\cos(7983t)$$
$$x_2 = 0.2834\cos(2505t) + 1.283\cos(7983t)$$

A potential problem with this approach is that, for additional degrees of freedom, the size of the matrix varies with the square of the number of coordinates. For example, we inverted a 2^2x2^2, or 4x4, complex matrix for our two degree of freedom system. For a three degree of freedom model, it would be necessary to invert a 3^2x3^2, or 9x9, complex matrix, and so on. While computational capabilities continually increase, modal analysis offers an alternative to this approach. The fundamental idea behind modal analysis is that a coordinate transformation is applied to convert from the model, or local, coordinate system into a modal coordinate system. While these modal coordinates do not have physical significance, they lead to uncoupled equations of motion because the off-diagonal terms in the mass and stiffness matrices are zero. The coordinate transformation is a diagonalization process and relies upon the orthogonality of the eigenvectors. Let's rework Example 1.3.1 to demonstrate the modal analysis approach.

> The fundamental idea behind modal analysis is that a transformation is applied to convert from a local into a modal coordinate system. The modal coordinates are then uncoupled.

Example 1.3.2: Free vibration by modal analysis

The first step in the modal analysis approach is typically to find the eigensolution (natural frequencies and mode shapes). However, we have already completed this step in the previous example. Our next task is to define the modal matrix, $[P]$. It is a square matrix whose columns are composed of the mode shapes, $[P] = [\psi_1 \quad \psi_2] = \begin{bmatrix} 0.8431 & -0.5931 \\ 1 & 1 \end{bmatrix}$, where we've continued with the decision to normalize to coordinate x_2 for illustrative purposes. As noted, the orthogonality conditions for eigenvectors enable us to diagonalize (i.e., make the off-diagonal terms zero) the mass and stiffness matrices and, therefore, uncouple the two equations of motion. The new mass and stiffness matrices in modal coordinates (identified by the q subscripts) are determined by premultiplying the mass and stiffness matrices in local coordinates by the transpose of the modal matrix and postmultiplying this product by the modal matrix.

$$[M_q]=[P]^T[M][P]=\begin{bmatrix}0.8431 & 1\\ -0.5931 & 1\end{bmatrix}\begin{bmatrix}1 & 0\\ 0 & 0.5\end{bmatrix}\begin{bmatrix}0.8431 & -0.5931\\ 1 & 1\end{bmatrix}=\begin{bmatrix}1.211 & 0\\ 0 & 0.8518\end{bmatrix}\text{ kg}$$

$$[K_q]=[P]^T[K][P]=\begin{bmatrix}0.8431 & 1\\ -0.5931 & 1\end{bmatrix}\begin{bmatrix}3\times10^7 & -2\times10^7\\ -2\times10^7 & 2\times10^7\end{bmatrix}\begin{bmatrix}0.8431 & -0.5931\\ 1 & 1\end{bmatrix}$$

$$[K_q]=\begin{bmatrix}7.601\times10^6 & 0\\ 0 & 5.4282\times10^7\end{bmatrix}\text{ N/m}$$

The two equations of motion can now be written in modal coordinates q_1 and q_2 using the matrix formulation: $[M_q]\{\ddot{q}\}+[K_q]\{q\}=\{0\}$. We see that the two equations are uncoupled and may be treated as separate single degree of freedom systems.

$$\begin{aligned}1.211\ddot{q}_1+7.601\times10^6 q_1&=0\\ 0.8518\ddot{q}_2+5.4282\times10^7 q_2&=0\end{aligned}$$

To use the solution techniques we developed in Section 1.1, we also need the initial conditions to be expressed in modal coordinates. Because the relationship between local and modal coordinates is $\{x\}=[P]\{q\}$, we can write $\{q\}=[P]^{-1}\{x\}$. To invert our 2x2 modal matrix, we switch the on-diagonal terms, change the sign of the off-diagonal terms, and divide each term by the scalar determinant, $|P|=P(1,1)P(2,2)-P(1,2)P(2,1)$.

$$[P]^{-1}=\frac{\begin{bmatrix}1 & 0.5931\\ -1 & 0.8431\end{bmatrix}}{0.8431\cdot1-(-0.5931)\cdot1}=\begin{bmatrix}0.6963 & 0.4130\\ -0.6963 & 0.5870\end{bmatrix}$$

We can then calculate the initial displacements $\{q_0\} = [P]^{-1}\{x_0\} = \begin{Bmatrix} 0.2833 \\ -1.283 \end{Bmatrix}$ mm and velocities $\{\dot{q}_0\} = [P]^{-1}\{\dot{x}_0\} = \begin{Bmatrix} 0 \\ 0 \end{Bmatrix}$ in modal coordinates.

We introduce here another general form for the solution of undamped free vibration given the initial displacement and velocity (in addition to the information provided in Section 1.1). The resulting displacement can be written as $x = \frac{\dot{x}_0}{\omega_n}\sin(\omega_n t) + x_0\cos(\omega_n t)$. Using this form, the modal displacements are $q_1 = 0\sin(2505t) + 0.2833\cos(2505t)$, which represents motion in the first natural frequency, and $q_2 = 0\sin(7983t) - 1.283\cos(7983t)$, which describes motion in the second natural frequency. To obtain the motion in local coordinates, we must perform the coordinate transformation $\{x\} = [P]\{q\} = \begin{bmatrix} 0.8431 & -0.5931 \\ 1 & 1 \end{bmatrix}\begin{Bmatrix} q_1 \\ q_2 \end{Bmatrix}$, which provides the relationships:

$$x_1 = 0.8431q_1 - 0.5931q_2 \text{ and}$$
$$x_2 = q_1 + q_2.$$

It should be emphasized that the x_2 vibration is determined simply by summing the modal displacements, q_1 and q_2. This is a direct outcome of normalizing our mode shapes to x_2 and is an important result for us. We will take advantage of the fact that the local response can be written as a sum of the modal contributions when we perform our modal fitting of measured FRFs. Also, we see that the x_1 motion is a linear combination of q_1 and q_2, where each modal response is scaled by the corresponding mode shape. Substitution of our q_1 and q_2 values into the previous equations for x_1 and x_2 yields the same result we obtained using the technique shown in Example 1.3.1, but the modal analysis approach did not require the inversion of the 2^2x2^2 complex matrix.

$$x_1 = 0.2388\cos(2505t) + 0.7610\cos(7983t)$$
$$x_2 = 0.2834\cos(2505t) + 1.283\cos(7983t)$$

Proportional damping means that all the coordinates pass through their equilibrium positions at the same instant for each mode shape. For low damping, this assumption is valid.

The final consideration in this section is solution of the two degree of freedom free vibration problem in the presence of damping. We've already stated that every physical system dissipates energy, so our analysis should incorporate the viscous damping matrix shown in Eq. 1.3.3. However, this complicates the eigensolution. At this point, we need to introduce the concept of proportional damping. Physically, proportional damping means that all the coordinates pass through their equilibrium (zero) positions at the same instant for each mode shape. For the low damping observed in the typical mechanical assemblies we will be considering, this assumption is realistic. For very high damping values, however, it is less reasonable because there may be significant phase differences between the motions of individual coordinates. Mathematically, proportional damping requires that the damping matrix can be written as a linear combination of the mass and stiffness matrices: $[C]=\alpha[M]+\beta[K]$, where α and β are real numbers.

Provided the proportional damping requirement is satisfied, then damping may be neglected in the eigensolution and the modal analysis procedure follows the steps provided in Example 1.3.2. The only modifications are that we must calculate the modal damping matrix $[C_q]=[P]^T[C][P]$ and the general solution to the uncoupled modal equations of motion $\lfloor M_q \rfloor\{\ddot{q}\}+\lfloor C_q \rfloor\{\dot{q}\}+\lfloor K_q \rfloor\{q\}=\{0\}$ is different. For the underdamped case, we can write $q=e^{-\zeta\omega_n t}\left(\frac{\dot{q}_0+\zeta\omega_n q_0}{\omega_d}\sin(\omega_d t)+q_0\cos(\omega_d t)\right)$. Otherwise, the solution proceeds as before.

1.4 Two degree of freedom forced vibration

We will use the two degree of freedom lumped parameter spring-mass-damper model shown in Fig. 1.3.1, but will impose external harmonic forces at coordinates x_1 and x_2 for the general case. See Fig. 1.4.1. However, for linear systems we can apply the principle of superposition to consider the forces separately and then sum the individual contributions. For demonstration purposes, we will consider only the $f_2e^{i\omega t}$ force applied to coordinate x_2. The equations of motion in matrix form for this system are:

$$\begin{bmatrix} m_1 & 0 \\ 0 & m_2 \end{bmatrix}\begin{Bmatrix} \ddot{x}_1 \\ \ddot{x}_2 \end{Bmatrix}+\begin{bmatrix} c_1+c_2 & -c_2 \\ -c_2 & c_2 \end{bmatrix}\begin{Bmatrix} \dot{x}_1 \\ \dot{x}_2 \end{Bmatrix}+\begin{bmatrix} k_1+k_2 & -k_2 \\ -k_2 & k_2 \end{bmatrix}\begin{Bmatrix} x_1 \\ x_2 \end{Bmatrix}=\begin{Bmatrix} 0 \\ f_2 \end{Bmatrix}. \qquad (1.4.1)$$

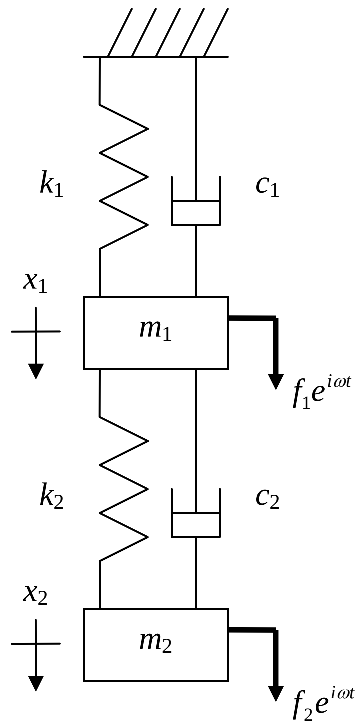

Figure 1.4.1: Two degree of freedom, lumped parameter system (damped with force).

By assuming solutions of the form $x_{1,2} = X_{1,2}e^{i\omega t}$ and substituting in Eq. 1.4.1, we obtain:

$$\left(-\omega^2[M]+i\omega[C]+[K]\right)\{X\}e^{i\omega t} = \{F\}e^{i\omega t}. \tag{1.4.2}$$

We have two methods that we can use to determine the steady state forced vibration response for this system. The first is modal analysis, which requires proportional damping, and the second is complex matrix inversion, which places no restrictions on the nature of the system damping. Let's begin with modal analysis.

Modal analysis

Our first step in the modal analysis approach is to write the system equations of motion in local coordinates as shown in Eq. 1.4.1; we continue to consider the f_2 case in this discussion.

Provided proportional damping exists (i.e., $[C] = \alpha[M] + \beta[K]$ is true), then we can ignore damping to find the eigensolution. Note that this solution is also independent of the external force(s). We find the eigenvalues (natural frequencies) and eigenvectors (modes shapes) using Eq. 1.3.4, $([M]s^2 + [K])\{X\}e^{st} = \{0\}$. The eigenvalues are determined from the roots of Eq. 1.3.5, $\left|[M]s^2 + [K]\right| = 0$. The natural frequencies are computed from $s_j^{\ 2} = -\omega_{nj}^{\ 2}$, j = 1 to 2 (the number of degrees of freedom). We can then use either of the equations of motion to find the 2x1 mode shapes for the two degree of freedom system:

$$\psi_1 = \begin{Bmatrix} \frac{X_1}{X_2}\left(s_1^{\ 2}\right) \\ 1 \end{Bmatrix} \text{ and } \psi_2 = \begin{Bmatrix} \frac{X_1}{X_2}\left(s_2^{\ 2}\right) \\ 1 \end{Bmatrix}, \tag{1.4.3}$$

where we have normalized to the location of the force application (coordinate x_2). Using the mode shapes, we assemble the 2x2 modal matrix $[P] = [\psi_1 \quad \psi_2]$. We can then use the modal matrix to transform into modal coordinates (and uncouple the equations of motion). The diagonal modal mass, damping, and stiffness matrices are: $[M_q] = [P]^T[M][P] = \begin{bmatrix} m_{q1} & 0 \\ 0 & m_{q2} \end{bmatrix}$, $[C_q] = [P]^T[C][P] = \begin{bmatrix} c_{q1} & 0 \\ 0 & c_{q2} \end{bmatrix}$, and $[K_q] = [P]^T[K][P] = \begin{bmatrix} k_{q1} & 0 \\ 0 & k_{q2} \end{bmatrix}$, respectively. We must also transform the local force vector into modal coordinates:

$$\{R\} = \begin{Bmatrix} R_1 \\ R_2 \end{Bmatrix} = [P]^T\{F\} = \begin{bmatrix} \frac{X_1}{X_2}\left(s_1^{\ 2}\right) & 1 \\ \frac{X_1}{X_2}\left(s_2^{\ 2}\right) & 1 \end{bmatrix} \begin{Bmatrix} 0 \\ f_2 \end{Bmatrix} = \begin{bmatrix} p_1 & 1 \\ p_2 & 1 \end{bmatrix} \begin{Bmatrix} 0 \\ f_2 \end{Bmatrix} = \begin{Bmatrix} f_2 \\ f_2 \end{Bmatrix}. \tag{1.4.4}$$

The modal equations of motion are:

$$\begin{aligned} m_{q1}\ddot{q}_1 + c_{q1}\dot{q}_1 + k_{q1}q_1 &= R_1 \\ m_{q2}\ddot{q}_2 + c_{q2}\dot{q}_2 + k_{q2}q_2 &= R_2 \end{aligned} \tag{1.4.5}$$

and the corresponding complex FRFs (steady state responses in the frequency domain) are:

$$\frac{Q_1}{R_1} = \frac{1}{k_{q1}}\left(\frac{\left(1-r_1^{\,2}\right)-i\left(2\zeta_{q1}r_1\right)}{\left(1-r_1^{\,2}\right)^2+\left(2\zeta_{q1}r_1\right)^2}\right) \text{ and } \frac{Q_2}{R_2} = \frac{1}{k_{q2}}\left(\frac{\left(1-r_2^{\,2}\right)-i\left(2\zeta_{q2}r_2\right)}{\left(1-r_2^{\,2}\right)^2+\left(2\zeta_{q2}r_2\right)^2}\right), \tag{1.4.6}$$

where $r_{1,2} = \frac{\omega}{\omega_{n1,2}}$ and $\zeta_{q1,2} = \frac{c_{q1,2}}{2\sqrt{k_{q1,2}m_{q1,2}}}$. We transform into local coordinates using $\{X\} = \begin{Bmatrix} X_1 \\ X_2 \end{Bmatrix} = [P]\{Q\} = \begin{bmatrix} p_1 & p_2 \\ 1 & 1 \end{bmatrix}\begin{Bmatrix} Q_1 \\ Q_2 \end{Bmatrix}$ so that $X_1 = p_1Q_1 + p_2Q_2$ and $X_2 = Q_1 + Q_2$.
Dividing each of these equations by F_2 gives the cross and direct FRFs for the f_2 force application, respectively. The cross FRF, which indicates that the force and measurement coordinates are not coincident, is:

$$\frac{X_1}{F_2} = \frac{p_1Q_1 + p_2Q_2}{F_2} = p_1\frac{Q_1}{F_2} + p_2\frac{Q_2}{F_2} = p_1\frac{Q_1}{R_1} + p_2\frac{Q_2}{R_2}, \tag{1.4.7}$$

where we see that the cross FRF is the sum of the modal FRFs scaled by the mode shapes (remember that $R_1 = R_2 = F_2$ from Eq. 1.4.4). The direct FRF, which denotes that the measurement is performed at the force input location, is:

$$\frac{X_2}{F_2} = \frac{Q_1 + Q_2}{F_2} = \frac{Q_1}{F_2} + \frac{Q_2}{F_2} = \frac{Q_1}{R_1} + \frac{Q_2}{R_2}. \tag{1.4.8}$$

We observe the important result that the direct FRF is simply the sum of the modal contributions. This is important for our subsequent analyses. Measurement of the frequency response functions on a physical system enable extraction of the model parameters and visualization of the natural frequencies and mode shapes.

Example 1.4.1: Forced vibration by modal analysis

Consider the chain-type, lumped parameter two degree of freedom system shown in Fig. 1.4.1. For the upper spring-mass-damper, the local coordinate constants are: $k_1 = 4\times10^5$ N/m, $c_1 = 80$ N-s/m, and $m_1 = 2$ kg. For the lower spring-mass-damper, the local coordinate constants are: $k_2 = 6\times10^5$ N/m, $c_2 = 120$ N-s/m, and $m_2 = 1$ kg. A harmonic force $f_2 = 100e^{i\omega t}$ N is applied to the lower mass (at coordinate x_2); we will not consider any force applied to the upper mass, although this force could be considered separately and the result added to the solution of the analysis we will perform here. The local mass, damping, and stiffness matrices are: $M = \begin{bmatrix} 2 & 0 \\ 0 & 1 \end{bmatrix}$ kg, $C = \begin{bmatrix} 200 & -120 \\ -120 & 120 \end{bmatrix}$ N-s/m, and $K = \begin{bmatrix} 1\times10^6 & -6\times10^5 \\ -6\times10^5 & 6\times10^5 \end{bmatrix}$ N/m, respectively. To use modal analysis, we must verify that proportional damping exists. For $\alpha = 0$ and $\beta = \frac{1}{5000}$, we see that the relationship $[C] = \alpha[M] + \beta[K]$ is satisfied. We can therefore determine the eigenvalues using:

$$\begin{vmatrix} 2s^2 + 1\times10^6 & -6\times10^5 \\ -6\times10^5 & s^2 + 6\times10^5 \end{vmatrix} = 0.$$

The two roots of the determinant are: $s_1^{\,2} = -122799.81$ (rad/s)^2 and $s_2^{\,2} = -977200.19$ (rad/s)^2, which gives the natural frequencies $\omega_{n1} = 350.43$ rad/s and $\omega_{n2} = 988.53$ rad/s ($\omega_{n1} < \omega_{n2}$). To determine the roots, we first write the characteristic equation: $(2s^2 + 1\times10^6)(s^2 + 6\times10^5) - (-6\times10^5)^2 = 0$, or after simplifying $2s^4 + 2.2\times10^6 s^2 + 2.4\times10^{11} = 0$. Because this equation is quadratic in s^2, we can find the roots $s_1^{\,2}$ and $s_2^{\,2}$ using the quadratic equation.

For the eigenvectors (mode shapes), we normalize to the location of the force application, coordinate x_2. Using the equation of motion for the top mass (arbitrarily selected), we obtain the required ratio $\frac{X_1}{X_2} = \frac{6\times10^5}{2s^2 + 1\times10^6}$. Substitution of $s_1^{\,2} = -122799.81$ (rad/s)^2 and $s_2^{\,2} = -977200.19$ (rad/s)^2 into Eq. 1.4.3 gives the two mode shapes $\psi_1 = \begin{Bmatrix} 0.7953 \\ 1 \end{Bmatrix}$ and $\psi_2 = \begin{Bmatrix} -0.6287 \\ 1 \end{Bmatrix}$, respectively. We can now construct the modal matrix:

$$[P] = [\psi_1 \quad \psi_2] = \begin{bmatrix} 0.7953 & -0.6287 \\ 1 & 1 \end{bmatrix}$$

and transform the local mass, stiffness, and damping matrices into modal coordinates:

$$[M_q] = [P]^T[M][P] = \begin{bmatrix} 2.265 & 0 \\ 0 & 1.790 \end{bmatrix} \text{ kg,}$$

$$[K_q] = [P]^T[K][P] = \begin{bmatrix} 2.782\times10^5 & 0 \\ 0 & 1.750\times10^6 \end{bmatrix} \text{ N/m, and}$$

$$[C_q] = [P]^T[C][P] = \begin{bmatrix} 55.63 & 0 \\ 0 & 349.9 \end{bmatrix} \text{ N-s/m.}$$

A simple check at this point is to recalculate the natural frequencies using the modal parameters. The results should match the eigenvalue solution. Here, we see that

$$\omega_{n1} = \sqrt{\frac{k_{q1}}{m_{q1}}} = \sqrt{\frac{2.782\times10^5}{2.265}} = 350.46 \text{ rad/s and } \omega_{n2} = \sqrt{\frac{k_{q2}}{m_{q2}}} = \sqrt{\frac{1.750\times10^6}{1.790}} = 988.76 \text{ rad/s,}$$

where the differences are due to round-off error, but the results are essentially the same. We can also determine the modal damping ratios:

$$\zeta_{q1} = \frac{c_{q1}}{2\sqrt{k_{q1}m_{q1}}} = \frac{55.63}{2\sqrt{2.782\times10^5 \cdot 2.265}} = 0.035 \text{ (3.5\% damping) and}$$

$$\zeta_{q2} = \frac{c_{q2}}{2\sqrt{k_{q2}m_{q2}}} = \frac{349.9}{2\sqrt{1.750\times10^6 \cdot 1.790}} = 0.099 \text{ (9.9\% damping).}$$

To write our uncoupled equations of motion in modal coordinates, we also need the modal force vector, which we obtain by substitution into Eq. 1.4.4.

$$\{R\} = \begin{bmatrix} 0.7953 & 1 \\ -0.6287 & 1 \end{bmatrix}\begin{Bmatrix} 0 \\ 100 \end{Bmatrix} = \begin{Bmatrix} 100 \\ 100 \end{Bmatrix} \text{ N}$$

$$2.265\ddot{q}_1 + 55.63\dot{q}_1 + 2.782\times10^5 q_1 = 100$$

$$1.790\ddot{q}_2 + 349.9\dot{q}_2 + 1.750\times10^6 q_2 = 100$$

The FRFs for the single degree of freedom modal systems are:

$$\frac{Q_1}{R_1} = \frac{1}{2.782\times10^5}\left(\frac{(1-r_1^2) - i(0.070r_1)}{(1-r_1^2)^2 + (0.070r_1)^2}\right) \text{ and } \frac{Q_2}{R_2} = \frac{1}{1.750\times10^6}\left(\frac{(1-r_2^2) - i(0.198r_2)}{(1-r_2^2)^2 + (0.198r_2)^2}\right),$$

where $r_1 = \frac{\omega}{350.43}$ and $r_2 = \frac{\omega}{988.53}$. The direct and cross FRFs are then $\frac{X_2}{F_2} = \frac{Q_1}{R_1} + \frac{Q_2}{R_2}$ and $\frac{X_1}{F_2} = 0.7953\frac{Q_1}{R_1} - 0.6287\frac{Q_2}{R_2}$, respectively. See Figs. 1.4.2 and 1.4.3. Because motion in the second mode shape, corresponding to $\omega_{n2} = 988.53$ rad/s, exhibits a 180 deg phase shift between the two coordinates (i.e., they are out of phase), the second mode is "inverted" in the cross FRF plot.

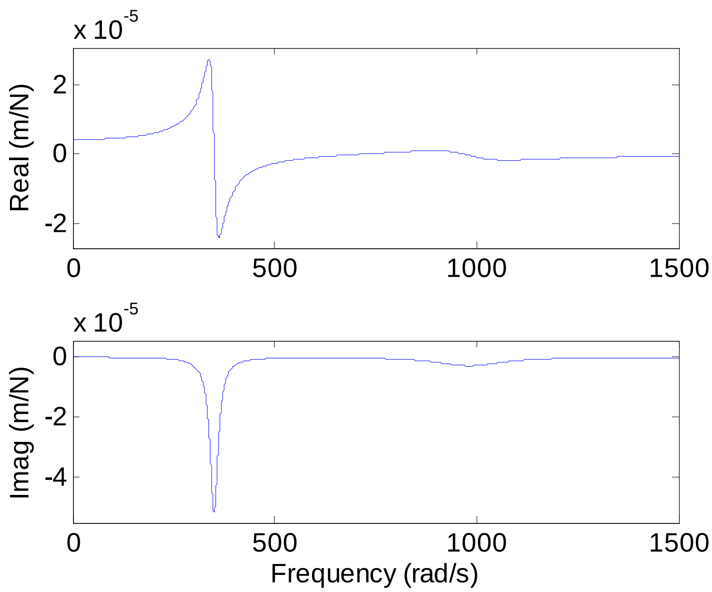

Figure 1.4.2: The real and imaginary parts of the direct FRF are determined from the sum of the modal contributions.

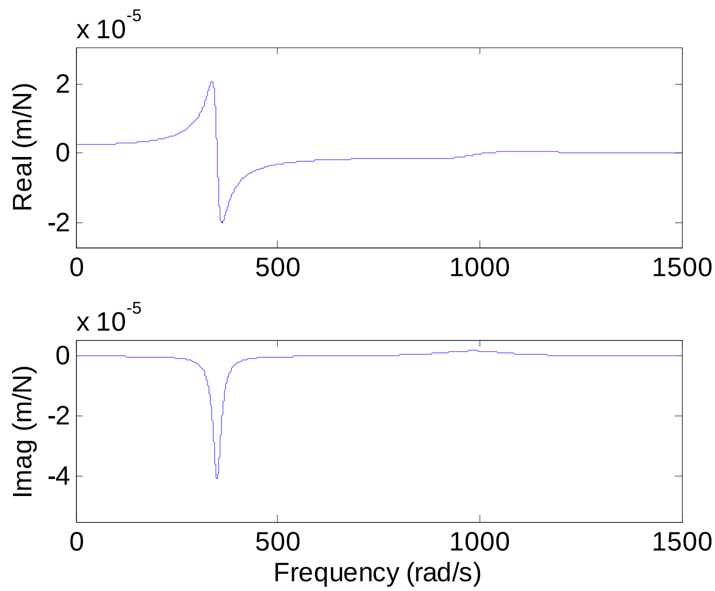

Figure 1.4.3: The real and imaginary parts of the cross FRF are obtained by scaling the two modes by the corresponding mode shape and summing the results.

Complex matrix inversion

Our final task of this section is to describe an alternative to modal analysis, referred to as complex matrix inversion. This approach does not require proportional damping, but does include the inversion of a 2x2 frequency dependent, complex matrix for the two degree of freedom system we are considering here. We'll first write Eq. 1.4.2 in the form $[A]\{X\}=\{F\}$, where $[A]=\begin{bmatrix} a_{11} & a_{12} \\ a_{21} & a_{22} \end{bmatrix}=\left(-\omega^2[M]+i\omega[C]+[K]\right)$. The two degree of freedom system has four FRFs that we'd like to determine. First, we have the direct and cross FRFs, $\frac{X_2}{F_2}$ and $\frac{X_1}{F_2}$, due to the force application at coordinate x_2 that we previously determined using modal analysis. Second, we have the direct and cross FRFs, $\frac{X_1}{F_1}$ and $\frac{X_2}{F_1}$, due to the force application at coordinate x_1. We did not explicitly show the modal solution to this case, but the only differences are that we would normalize the mode shapes to x_1 and the FRFs would then be computed from $\frac{X_1}{F_1} = \frac{Q_1}{R_1} + \frac{Q_2}{R_2}$ and $\frac{X_2}{F_1} = p_1 \frac{Q_1}{R_1} + p_2 \frac{Q_2}{R_2}$, where $P = \begin{bmatrix} 1 & 1 \\ p_1 & p_2 \end{bmatrix}$ would be used to determine the modal mass, stiffness, and damping matrices.

Rewriting $[A]\{X\} = \{F\}$ as $\{X\}\{F\}^{-1} = [A]^{-1}$ provides all four FRFs. They are ordered as: $\begin{Bmatrix} \frac{X_1}{F_1} & \frac{X_1}{F_2} \\ \frac{X_2}{F_1} & \frac{X_2}{F_2} \end{Bmatrix} = \begin{bmatrix} b_{11} & b_{12} \\ b_{21} & b_{22} \end{bmatrix}$, where we've used the b_{ij} notation to indicate the individual terms in the inverted $[A]$ matrix. In our analysis, $[A]$ is symmetric. Therefore, $b_{12} = b_{21}$ and $\frac{X_1}{F_2} = \frac{X_2}{F_1}$. This condition is referred to as reciprocity. Physically, it means that we get the same result if we: 1) excite the system at coordinate x_2 and measure the response at x_1, as if we: 2) excite the system at coordinate x_1 and measure the response at x_2.

Reciprocity means that we get the same FRF if we: 1) excite at coordinate *i* and measure at coordinate *j*; or 2) if we excite at *j* and measure at *i*.

For the two degree of freedom system, we can directly write the individual terms in $[A]^{-1}$ as:

$$[A]^{-1} = \frac{\begin{bmatrix} a_{22} & -a_{12} \\ -a_{21} & a_{11} \end{bmatrix}}{a_{11} \cdot a_{22} - a_{12} \cdot a_{21}} = \frac{\begin{bmatrix} -\omega^2 m_2 + i\omega c_2 + k_2 & i\omega c_2 + k_2 \\ i\omega c_2 + k_2 & -\omega^2 m_1 + i\omega(c_1 + c_2) + k_1 + k_2 \end{bmatrix}}{a_{11} \cdot a_{22} - a_{12} \cdot a_{21}}.$$

For example, $\frac{X_1}{F_1} = b_{11} = \frac{-\omega^2 m_2 + i\omega c_2 + k_2}{a_{11} \cdot a_{22} - a_{12} \cdot a_{21}}$. Note that this complex expression is a function of the forcing frequency ω so it must be evaluated over the desired frequency range in order to produce plots equivalent to those obtained for the modal analysis example.

1.5 System identification

The previous section describes the modal analysis steps required to obtain the direct and cross FRFs in local coordinates given a system model (we treated the chain-type, lumped parameter case, but other model geometries could be considered as well). This approach required that the mass, damping, and stiffness matrices be known. However, this is not the case for arbitrary structures. Our actual task is typically to measure the FRFs for the system of interest and then define a model by performing a modal fit to the measured data.

Modal fitting

Our fitting approach will be a "peak picking" method where we use the real and imaginary parts of the system FRFs to identify the modal parameters [6]. This approach works well provided the system modes are not closely spaced. However, even if two modeled modes are relatively close in frequency, we can still obtain a reasonable modal fit as we'll see in Example 1.5.1.

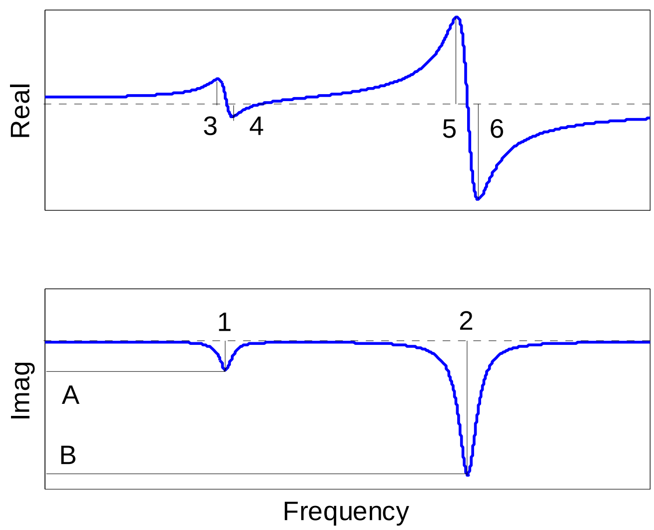

Figure 1.5.1: Two degree of freedom direct FRF with the frequencies and amplitudes required for peak picking identified.

To demonstrate the fitting steps, consider the direct FRF shown in Fig. 1.5.1. This FRF clearly has two modes within the measurement bandwidth. To determine the modal parameters which populate the 2x2 modal matrices, we must identify three frequencies and one peak value for each mode. [Note that we have automatically assumed proportional damping in using this approach. Additionally, if there were three dominant modes we wished to model, we would obtain 3x3 modal matrices and so on.] The frequencies labeled 1 and 2 along the horizontal frequency axis in the imaginary part of the direct FRF (Fig. 1.5.1) correspond to the minimum imaginary peaks and provide the two natural frequencies, ω_{n1} and ω_{n2}, respectively. The difference between frequencies 4 and 3, labeled along the frequency axis of the real part of the direct FRF, is used to determine the modal damping ratio for the first mode, ζ_{q1}:

$$\omega_4 - \omega_3 = \omega_{n1}(1+\zeta_{q1}) - \omega_{n1}(1-\zeta_{q1}) = 2\zeta_{q1}\omega_{n1} \text{ or } \zeta_{q1} = \frac{\omega_4 - \omega_3}{2\omega_{n1}}. \quad (1.5.1)$$

Similarly, the difference between frequencies 6 and 5 is used to determine ζ_{q2}:

$$\zeta_{q2} = \frac{\omega_6 - \omega_5}{2\omega_{n2}}. \quad (1.5.2)$$

The (negative) peak value, *A*, identified along the vertical axis of the imaginary part of the direct FRF is next used to find the modal stiffness value, k_{q1}:

$$A = \frac{-1}{2k_{q1}\zeta_{q1}} \text{ or } k_{q1} = \frac{-1}{2\zeta_{q1}A}. \quad (1.5.3)$$

Similarly, the peak value *B* is used to determine k_{q2}:

$$k_{q2} = \frac{-1}{2\zeta_{q2}B}. \quad (1.5.4)$$

At this point, we can directly populate the modal stiffness matrix $[K_q] = \begin{bmatrix} k_{q1} & 0 \\ 0 & k_{q2} \end{bmatrix}$.

However, we must calculate the modal mass and damping values from the additional information we've obtained. We determine the modal masses using the natural frequencies and modal stiffness values:

$$\omega_{n1} = \sqrt{\frac{k_{q1}}{m_{q1}}} \text{ or } m_{q1} = \frac{k_{q1}}{\omega_{n1}{}^2} \text{ and } m_{q2} = \frac{k_{q2}}{\omega_{n2}{}^2}. \quad (1.5.5)$$

The modal damping coefficients are computed using the modal damping ratios, stiffness values, and masses:

$$\zeta_{q1} = \frac{c_{q1}}{2\sqrt{k_{q1}m_{q1}}} \text{ or } c_{q1} = 2\zeta_{q1}\sqrt{k_{q1}m_{q1}} \text{ and } c_{q2} = 2\zeta_{q2}\sqrt{k_{q2}m_{q2}}\,. \tag{1.5.6}$$

We can now write the remaining modal matrices $[M_q] = \begin{bmatrix} m_{q1} & 0 \\ 0 & m_{q2} \end{bmatrix}$ and $[C_q] = \begin{bmatrix} c_{q1} & 0 \\ 0 & c_{q2} \end{bmatrix}$.

To complete this discussion, we will detail the steps necessary to define a chain-type, lumped parameter model based on measured FRFs. Before continuing with the model definition, let's carry out an example of peak picking to determine the modal matrices.

Example 1.5.1: Peak picking modal fit

Figure 1.5.2 shows an example FRF that could be obtained from a tool point measurement. Our task is to perform a modal fit to identify the modal mass, damping, and stiffness matrices. The first step is to decide how many modes we wish to fit. A visual inspection of the FRF shows that a three mode fit is appropriate. The three natural frequencies are identified by locating the three minimum peaks of the imaginary part and recording the associated frequencies. These are identified as 499 Hz, 761 Hz, and 849 Hz in Fig. 1.5.3. We determine the modal damping ratios using the frequencies of the local maximum and minimum values of the real part according to Eq. 1.5.1. These are shown as 460 Hz and 533 Hz for mode 1; 726 Hz and 787 Hz for mode 2; and 827 Hz and 873 Hz for mode 3. The modal damping ratios are then:

$$\zeta_{q1} = \frac{533-460}{2\cdot 499} = 0.073\,,\ \zeta_{q2} = \frac{787-726}{2\cdot 761} = 0.040\,,\text{ and } \zeta_{q3} = \frac{873-827}{2\cdot 849} = 0.027\,.$$

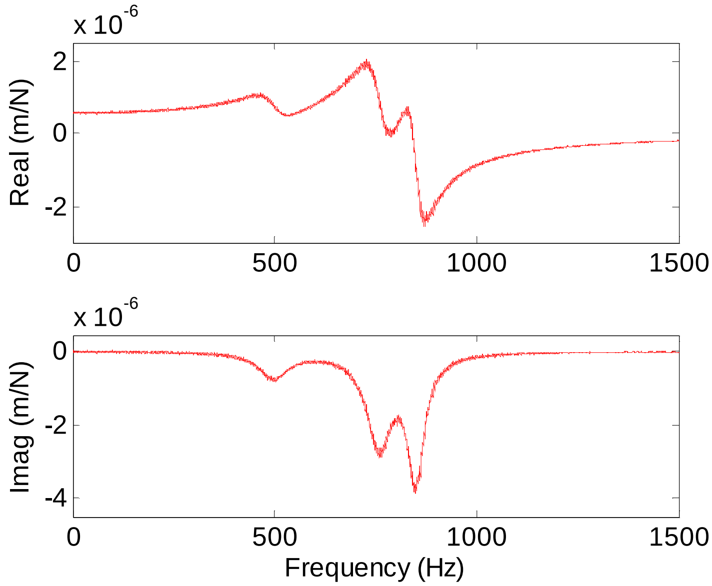

Figure 1.5.2: Example tool point FRF for peak picking exercise.

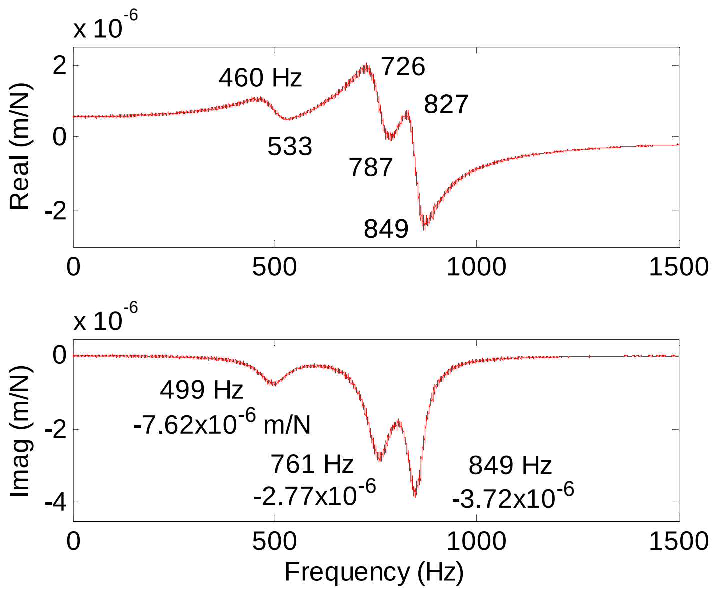

Figure 1.5.3: Three degree of freedom peak picking example with required frequencies and amplitudes identified.

The imaginary part negative peak values for each mode are also listed in Fig. 1.5.3. The modal stiffness values are calculated using Eq. 1.5.3.

$$k_{q1} = \frac{-1}{2 \cdot 0.073 \cdot \left(-7.62 \times 10^{-7}\right)} = 8.99 \times 10^{6} \text{ N/m}$$

$$k_{q2} = \frac{-1}{2 \cdot 0.040 \cdot \left(-2.77 \times 10^{-6}\right)} = 4.51 \times 10^{6} \text{ N/m}$$

$$k_{q3} = \frac{-1}{2 \cdot 0.027 \cdot \left(-3.72 \times 10^{-6}\right)} = 4.98 \times 10^{6} \text{ N/m}$$

We find the modal masses using Eq. 1.5.5. We must be sure to pay special attention to units for these calculations; note that we have switched from frequency units of Hz to rad/s by multiplying by 2π and the stiffness values are expressed in N/m.

$$m_{q1} = \frac{8.99 \times 10^{6}}{(499 \cdot 2\pi)^2} = 0.914 \text{ kg} \qquad m_{q2} = \frac{4.51 \times 10^{6}}{(761 \cdot 2\pi)^2} = 0.197 \text{ kg}$$

$$m_{q3} = \frac{4.98 \times 10^{6}}{(849 \cdot 2\pi)^2} = 0.175 \text{ kg}$$

Finally, the modal damping coefficients are determined using Eq. 1.5.6. Again, units compatibility should be ensured. In the following calculations, stiffness and mass values are expressed in N/m and kg, respectively, to obtain damping coefficient units of N-s/m.

$$c_{q1} = 2 \cdot 0.073\sqrt{8.99 \times 10^{6} \cdot 0.914} = 419 \text{ N-s/m}$$

$$c_{q2} = 2 \cdot 0.040\sqrt{4.51 \times 10^{6} \cdot 0.197} = 75.4 \text{ N-s/m}$$

$$c_{q3} = 2 \cdot 0.027\sqrt{4.98 \times 10^{6} \cdot 0.175} = 50.4 \text{ N-s/m}$$

The 3x3 modal matrices can now be written as:

$$\left[M_q\right] = \begin{bmatrix} 0.914 & 0 & 0 \\ 0 & 0.197 & 0 \\ 0 & 0 & 0.175 \end{bmatrix} \text{ kg}, \ \left[C_q\right] = \begin{bmatrix} 419 & 0 & 0 \\ 0 & 75.4 & 0 \\ 0 & 0 & 50.4 \end{bmatrix} \text{ N-s/m, and}$$

$$[K_q]=\begin{bmatrix} 8.99\times10^6 & 0 & 0 \\ 0 & 4.51\times10^6 & 0 \\ 0 & 0 & 4.98\times10^6 \end{bmatrix} \text{ N/m.}$$

The individual modal contributions may be described using Eq. 1.5.6:

$$\frac{Q_j}{R_j}=\frac{1}{k_{qj}}\left(\frac{(1-r_j^{\,2})-i(2\zeta_{qj}r_j)}{(1-r_j^{\,2})^2+(2\zeta_{qj}r_j)^2}\right),$$

where $r_j=\frac{\omega}{\omega_{nj}}$, j = 1 to 3. The individual modes are plotted, together with the original FRF, in Fig. 1.5.4. As we've discussed, however, the direct FRF in local (physical) coordinates is the sum of the modal contributions so we may simply add the individual modal responses on a frequency by frequency basis to define our final fit. This result is shown in Fig. 1.5.5.

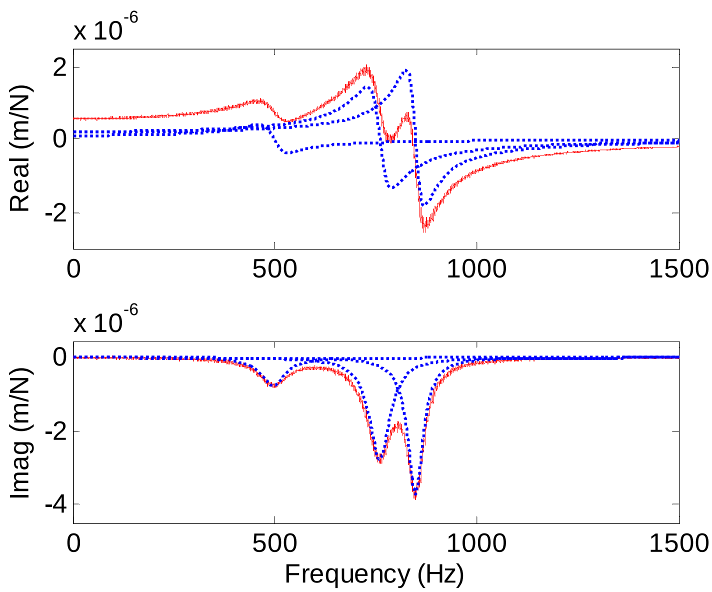

Figure 1.5.4: Example tool point and three modal coordinate FRFs determined by peak picking approach.

For this contrived example, the original modal parameters used to construct the "measured" FRF are known. Therefore, we can compare our modal approximation to the true values. These results are provided in Table 1.5.1.

Table 1.5.1: True modal parameters and values obtained by peak picking modal fit.

	Mode 1		Mode 2		Mode 3	
	True	Fit	True	Fit	True	Fit
f_n (Hz)	500	499	760	761	850	849
ζ_q	0.090	0.073	0.050	0.040	0.030	0.027
k_q (N/m)	8.00×10^6	8.99×10^6	4.00×10^6	4.51×10^6	5.00×10^6	4.98×10^6

Model definition

Once we have determined the modal matrices by peak picking, the next step in defining a model is to use the measured direct and cross FRFs to find the mode shapes and construct the modal matrix. We'll again assume that the measured direct FRF, shown in Fig. 1.5.1, can be approximated with a two mode fit. This means that our model will have two degrees of freedom. As we've seen, for a two degree of freedom model, the mode shapes are 2x1 vectors so that the square modal matrix has dimensions of 2x2. Because the mode shapes have just two entries (one of which is 1), we only require one cross FRF to determine the second entry. As before, we can choose the coordinate to which we normalize our mode shapes for the model shown in Fig. 1.4.1. Let's define the coordinate of interest as x_2 so that the form of the modal matrix is $[P]=\begin{bmatrix} p_1 & p_2 \\ 1 & 1 \end{bmatrix}$. We determine p_1 and p_2 using: 1) the peak imaginary part values denoted *C*, corresponding to the first mode with the natural frequency ω_{n1}, and *D*, the second mode with the natural frequency ω_{n2}, in the cross FRF[2] shown in Fig. 1.5.6, together with: 2) the *A* and *B* values identified in Fig. 1.5.1.

[2] We observe that the cross FRF in Fig. 1.5.6 looks very different than the direct FRF in Fig. 1.5.1; the higher frequency mode is "upside down" in Fig. 1.5.6. As we saw in Section 1.4, this is because the two modes are out of phase for the cross FRF, which results in the sign change.

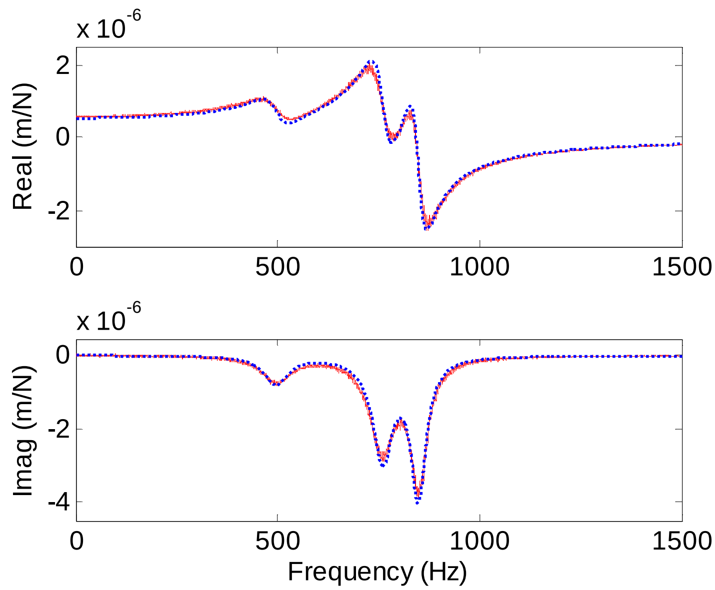

Figure 1.5.5: Example tool point FRF with three degree of freedom modal fit obtained by peak picking.

$$\frac{C}{A}=\frac{\dfrac{-p_1}{2k_{q1}\zeta_{q1}}}{\dfrac{-1}{2k_{q1}\zeta_{q1}}}=p_1 \text{ and } \frac{D}{B}=\frac{\dfrac{-p_2}{2k_{q2}\zeta_{q2}}}{\dfrac{-1}{2k_{q2}\zeta_{q2}}}=p_2 \tag{1.5.7}$$

We have used the ratio of the peak of the cross FRF to the direct FRF in each mode to determine the mode shapes because, as we discussed previously, the cross FRF can be expressed as the sum of the modal contributions with each mode scaled by the corresponding system mode shape. See Eq. 1.4.7. Once we have defined the modal matrix, we can determine the model parameters in local coordinates using the transformations (from modal to local coordinates) in Eqs. 1.5.8-1.5.10. The forms of $[M]$, $[C]$, and $[K]$ correspond to the pre-selected two degree of freedom chain-type, lumped parameter model.

$$[P]^{-T}\left[M_q\right][P]^{-1}=[M]=\begin{bmatrix} m_1 & 0 \\ 0 & m_2 \end{bmatrix} \tag{1.5.8}$$

$$[P]^{-T}[C_q][P]^{-1} = [C] = \begin{bmatrix} c_1 + c_2 & -c_2 \\ -c_2 & c_2 \end{bmatrix} \tag{1.5.9}$$

$$[P]^{-T}[K_q][P]^{-1} = [K] = \begin{bmatrix} k_1 + k_2 & -k_2 \\ -k_2 & k_2 \end{bmatrix} \tag{1.5.10}$$

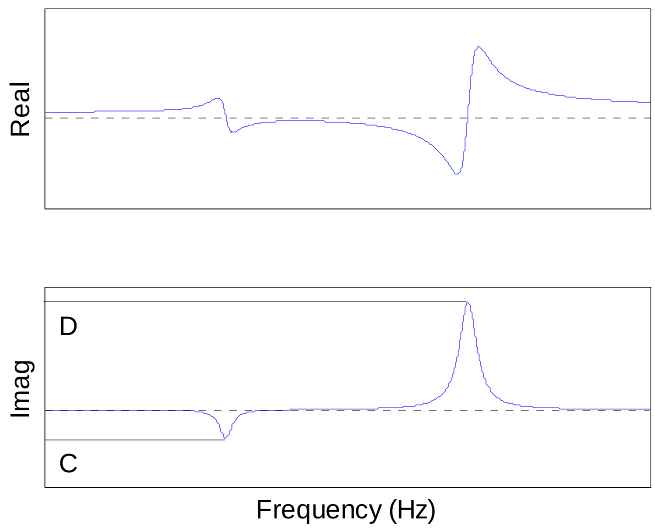

Figure 1.5.6: Two degree of freedom cross FRF with the amplitudes required for model development identified.

As a final note regarding model definition, it should be emphasized that if the measured direct FRF has three modes that we wish to model, then the square modal matrix will have dimensions of 3x3. To determine the modal matrix, we must measure, at minimum, two cross FRFs to give the two ratios required for the 3x1 mode shapes. Additional cross FRF measurements may be necessary to find measurement locations with good signal to noise ratio (i.e., away from system nodes, or locations of zero vibration amplitude regardless of the force input level).

Modal truncation

Prior to describing modal testing equipment, there is one remaining issue to highlight regarding modal fitting. Because FRF measurements always have a finite frequency range and elastic bodies possess an infinite number of degrees of freedom, there are necessarily modes that exist outside the measurement range. We typically measure from zero to a few of kHz at most (perhaps up to 10 kHz for a small mass impact hammer with a steel tip – see Section 1.6). However, omitting these higher frequency modes during peak picking affects the accuracy of the modal fit, particularly the real part of the FRF. Equations 1.2.6 and 1.2.7, which describe the real and imaginary parts of a single degree of freedom FRF, are reproduced here to demonstrate the effect.

$$\mathrm{Re}\left(\frac{X}{F}\right) = \frac{1}{k}\left(\frac{1-r^2}{\left(1-r^2\right)^2 + \left(2\zeta r\right)^2}\right) \tag{1.5.11}$$

$$\mathrm{Im}\left(\frac{X}{F}\right) = \frac{1}{k}\left(\frac{-2\zeta r}{\left(1-r^2\right)^2 + \left(2\zeta r\right)^2}\right) \tag{1.5.12}$$

It is seen that when the frequency ratio $r = \frac{\omega}{\omega_n}$ is large, or the driving frequency ω is very high and outside the measurement range, the denominator within the right parenthetical terms in these two equations becomes very large and the response approaches zero. This is seen at the right hand side of Fig. 1.2.4, for example. However, as r approaches zero, the parenthetical term in the real part approaches one and the parenthetical term in the imaginary part approaches zero. Therefore, the value of the real part approaches $\frac{1}{k}$ as r approaches zero[3]. If there are modes beyond the measurement bandwidth, neglecting these terms and the associated $\frac{1}{k}$ contributions leads to errors in the vertical location of the modal fit's real part. This is demonstrated in Ex. 1.5.2.

Example 1.5.2: High frequency mode truncation during modal fitting

A "measured" FRF is provided in Fig. 1.5.7. We will presume that the measurement bandwidth was 2 kHz, although a 5 kHz frequency range is shown for demonstration purposes. Within the 2 kHz range, two modes are visible and peak picking can be applied to determine the associated modal parameters. Using the values from the figure, the modal stiffness, mass, and damping matrix terms may be determined as shown in Ex. 1.5.1.

[3] This $\frac{1}{k}$ term can be referred to as the DC compliance.

$$\zeta_{q1} = \frac{393-356}{2\cdot 375} = 0.049 \qquad \zeta_{q2} = \frac{1122-1078}{2\cdot 1100} = 0.020$$

$$k_{q1} = \frac{-1}{2\cdot 0.049\cdot\left(-6.74\times 10^{-7}\right)} = 1.50\times 10^{7}\ \text{N/m}$$

$$k_{q2} = \frac{-1}{2\cdot 0.020\cdot\left(-6.26\times 10^{-6}\right)} = 3.99\times 10^{6}\ \text{N/m}$$

$$m_{q1} = \frac{1.50\times 10^{7}}{(375\cdot 2\pi)^2} = 2.70\ \text{kg} \qquad m_{q2} = \frac{3.99\times 10^{6}}{(1100\cdot 2\pi)^2} = 0.084\ \text{kg}$$

$$c_{q1} = 2\cdot 0.049\sqrt{1.50\times 10^{7}\cdot 2.70} = 624\ \text{N-s/m}$$

$$c_{q2} = 2\cdot 0.020\sqrt{3.99\times 10^{6}\cdot 0.084} = 23.2\ \text{N-s/m}$$

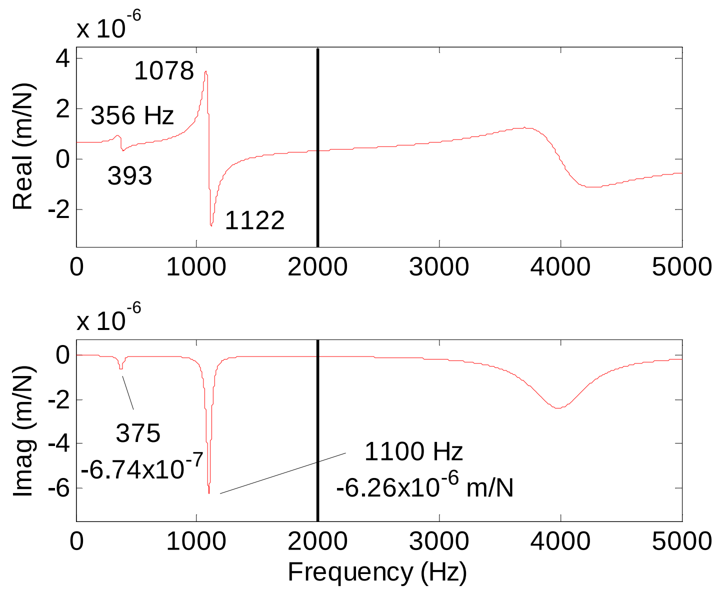

Figure 1.5.7: “Measured” direct FRF for Ex. 1.5.2. The peak picking values are listed within the 2 kHz measurement bandwidth. A 5 kHz frequency range is provided to show the truncated 4000 Hz mode.

The fit to the measured direct FRF is determined by summing the two contributions in modal coordinates according to:

$$\frac{X}{F} = \frac{Q_1}{R_1} + \frac{Q_2}{R_2} = \frac{1}{k_{q1}}\left(\frac{\left(1-r_1^{\ 2}\right) - i\left(2\zeta_{q1}r_1\right)}{\left(1-r_1^{\ 2}\right)^2 + \left(2\zeta_{q1}r_1\right)^2}\right) + \frac{1}{k_{q2}}\left(\frac{\left(1-r_2^{\ 2}\right) - i\left(2\zeta_{q2}r_2\right)}{\left(1-r_2^{\ 2}\right)^2 + \left(2\zeta_{q2}r_2\right)^2}\right),$$

where $r_1 = \frac{f}{375}$ and $r_2 = \frac{f}{1100}$ and f is given in Hz. It is seen in Fig. 1.5.8 that, although the shape of the two modes within the 2 kHz bandwidth are correctly identified, there is a noticeable offset in the real part of the fit. It appears too stiff (i.e., it is located below the measured FRF) because the DC compliance due to the 4000 Hz mode has not been considered. Because this mode is outside the measurement frequency range, it is not possible to fit the mode and determine the appropriate modal parameters. However, given the visible offset in Fig. 1.5.8, the combined contributions of truncated modes can be included by adding an effective DC compliance term to the fit. Specifically, for this example, the fit could be rewritten as:

$$\frac{X}{F} = \frac{1}{k} + \frac{Q_1}{R_1} + \frac{Q_2}{R_2},$$

where the $\frac{Q_j}{R_j}$ terms (j = 1, 2) are obtained through peak picking as described previously and the $\frac{1}{k}$ value is selected to move the fit to a vertical overlap with the measured FRF. If a value of $k = 3\times10^6$ N/m is applied here, the fit is improved and the result shown in Fig. 1.5.9 is obtained. Note that this stiffness value is equal to the modal stiffness of the 4000 Hz mode shown in Fig. 1.5.7 (for completeness, the modal damping ratio for this mode is 0.07).

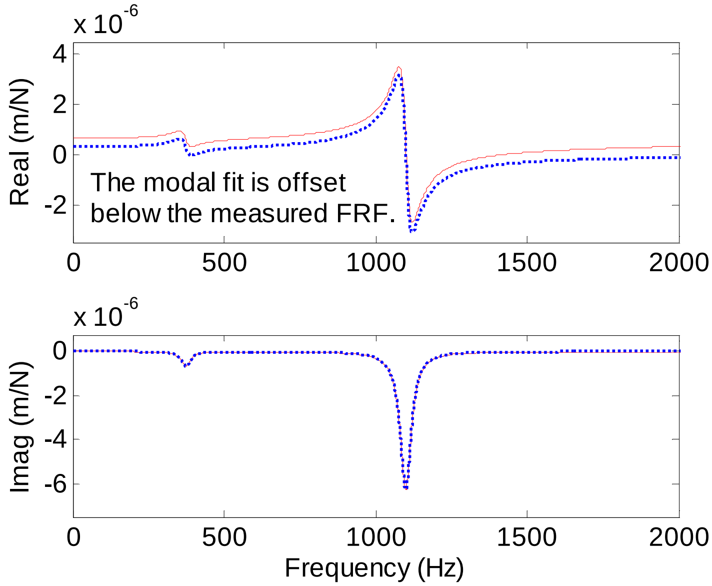

Figure 1.5.8: Result of modal fitting. An offset in the Re part of the fit (dotted line) is observed because the DC compliance of the 4000 Hz mode is not included.

1.6 Modal testing equipment

The basic hardware required to measure FRFs is:

- a mechanism for known force input across the desired frequency range;
- a transducer for vibration measurement, again with the required bandwidth; and
- a dynamic signal analyzer to record the time domain force and vibration inputs and convert these into the desired FRF.

The dynamic signal analyzer includes input channels for the time domain force and vibration signals and computes the Fourier transform of these signals to convert them to the frequency domain. It then calculates the ratio of the frequency domain vibration signal to the frequency domain force signal; this ratio is the FRF. The form of the FRF depends on the vibration transducer type and can be expressed as:

- receptance/compliance – the ratio of displacement to force (considered in the previous sections);
- mobility – the ratio of velocity to force; and
- inertance/accelerance – the ratio of acceleration to force.

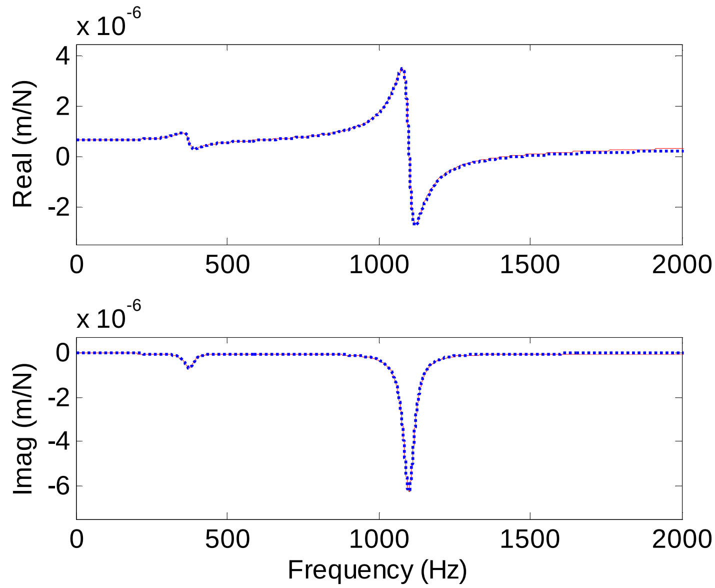

Figure 1.5.9: Result of modal fitting with the addition of a DC compliance term to correct for the truncated mode.

Force input

Common types of force excitation include:

- fixed frequency sine wave – The complex response is determined one frequency at a time with averaging occurring at each frequency over a short time interval. This is referred to as a sine sweep test.
- random signal – The frequency content of the random signal may be broadband (white noise) or truncated to a desired range (pink noise). Averaging over a fixed period of time is again applied.
- impulse – A short duration impact is used to excite the structure. This approach enables a broad range of frequencies to be excited in a single, short test. Multiple tests are typically averaged in the frequency domain to improve coherence, or the correlation between the force and vibration signals.

Common force input hardware includes:

- shaker – These systems include a harmonically driven armature and a base. The armature may be actuated along its axis by a magnetic coil or hydraulic force. The magnetic coil, or electrodynamic, configurations can provide excitation frequencies of tens of kHz with force levels from tens to thousands of N (increased force typically means a lower frequency range). Hydraulic shakers offer high force with the potential for a static preload, but relatively lower frequency ranges. In either case, the force is often applied to the structure of interest through a “stinger”, or a slender rod that supports axial tension and compression, but not bending or shear. A load cell is often incorporated in the setup to measure the input force. One consideration is that this load cell adds mass to the system under test, which can alter the FRF for low mass structures. Finally, the shaker must be isolated from the structure to prevent reaction forces due to the shaker motion from being transmitted through the shaker base to the structure. See Fig. 1.6.1.

Figure 1.6.1: Shaker example. The stinger is shown extending from the top end [7].

Figure 1.6.2: Example impact hammer. Many sizes and tip types are available. A medium sized hammer (0.32 kg) is shown [8].

- impact hammer – An impact hammer incorporates a force transducer in a metal, plastic, or rubber tip to measure the force input during a hammer strike. Because the setup and measurement time is short, it is a popular choice for tool-holder testing (referred to as impact testing). Naturally, the energy input to the structure is a function of the hammer mass; therefore, many sizes are available. Also, the bandwidth of the force input depends on the mass and tip stiffness. Stiffer tips tend to excite a wider frequency range, but also spread the input energy over this wider range. Softer tips concentrate the energy over a lower frequency range. Hard, plastic tips are a common choice for tool testing because they do not damage the cutting edge and generally provide sufficient excitation bandwidth. See Fig. 1.6.2.

Figure 1.6.3: Example accelerometer with 10 mg mass and 0.5 Hz to 5 kHz measurement bandwidth. Many sizes are available for various applications [9].

Vibration measurement

Vibration transducers are available in both non-contact and contact types. While non-contact transducers, such as capacitance probes and laser vibrometers, are preferred because they do not influence the system dynamics, contacting types, such as accelerometers, are more convenient to implement. As a compromise, low mass accelerometers are often used. See Fig. 1.6.3. In most applications, the addition of a few grams or less of accelerometer mass does not appreciably alter the response and the accelerometer can be attached using wax and then easily removed. Because accelerometers produce a signal which is proportional to acceleration, the inertance FRF is obtained. However, to convert from inertance, or $\frac{A}{F}$, to receptance, $\frac{X}{F}$, we can use the relationship:

$$\frac{X}{F} = -\frac{1}{\omega^2} \cdot \frac{A}{F}, \qquad (1.6.1)$$

which follows from the harmonic solution, $x = Xe^{i\omega t}$, and its second time derivative $\ddot{x} = -\omega^2 Xe^{i\omega t} = -\omega^2 x$. Equation 1.6.1 effectively describes double numerical integration in the frequency domain.

References

1. http://en.wikipedia.org/wiki/Modal_analysis, accessed July, 2008.
2. http://en.wikipedia.org/wiki/Tacoma_Narrows_Bridge, accessed July, 2008.
3. Inman, D., 2001, Engineering Vibration, 2nd Ed., Prentice Hall, Upper Saddle River, NJ, Section 1.10.
4. Thomson, W. and Dahleh, M., 1998, Theory of Vibration with Application, 5th Ed., Prentice Hall, Upper Saddle River, NJ, Section 3.9.
5. Leon, J., 1994, Linear Algebra with Applications, 4th Ed., Prentice Hall, Englewood Cliffs, NJ, Section 5.6.
6. Ewins, D., 2000, Modal Testing: Theory, Practice, and Application, 2nd Ed., Taylor & Francis, London.
7. http://www.modalshop.com/test_tmproducts.asp?ID=164, accessed July, 2008.
8. http://www.pcb.com/spec_sheet.asp?model=086D05&item_id=10517, accessed July, 2008.
9. http://www.pcb.com/spec_sheet.asp?model=338C24&item_id=2009, accessed July, 2008.